Geosci. Model Dev., 7, 981–999, 2014
www.geosci-model-dev.net/7/981/2014/
doi:10.5194/gmd-7-981-2014

Geoscientific Model Development
Open Access

Modelling methane emissions from natural wetlands by development and application of the TRIPLEX-GHG model

Q. Zhu[1,3], J. Liu[2], C. Peng[3,1], H. Chen[1,3], X. Fang[4,3], H. Jiang[5], G. Yang[1], D. Zhu[3], W. Wang[3], and X. Zhou[3]

[1]State Key Laboratory of Soil Erosion and Dryland Farming on the Loess Plateau, Northwest A&F University, Yangling 712100, China
[2]Contractor, Western Geographic Science Center, U.S. Geological Survey, Menlo Park, CA 94025, USA
[3]Center of CEF/ESCER, Department of Biological Science, University of Quebec at Montreal, Montreal H3C 3P8, Canada
[4]School of Earth Science and Engineering, Hohai University, Nanjing 210098, China
[5]International Institute for Earth System Science, Nanjing University, Hankou Road 22, Nanjing 210093, China

Correspondence to: C. Peng (peng.changhui@uqam.ca) and Q. Zhu (qiuan.zhu@gmail.com)

Received: 31 August 2013 – Published in Geosci. Model Dev. Discuss.: 4 November 2013
Revised: 27 February 2014 – Accepted: 31 March 2014 – Published: 26 May 2014

Abstract. A new process-based model TRIPLEX-GHG was developed based on the Integrated Biosphere Simulator (IBIS), coupled with a new methane (CH_4) biogeochemistry module (incorporating CH_4 production, oxidation, and transportation processes) and a water table module to investigate CH_4 emission processes and dynamics that occur in natural wetlands. Sensitivity analysis indicates that the most sensitive parameters to evaluate CH_4 emission processes from wetlands are r (defined as the CH_4 to CO_2 release ratio) and Q_{10} in the CH_4 production process. These two parameters were subsequently calibrated to data obtained from 19 sites collected from approximately 35 studies across different wetlands globally. Being heterogeneously spatially distributed, r ranged from 0.1 to 0.7 with a mean value of 0.23, and the Q_{10} for CH_4 production ranged from 1.6 to 4.5 with a mean value of 2.48. The model performed well when simulating magnitude and capturing temporal patterns in CH_4 emissions from natural wetlands. Results suggest that the model is able to be applied to different wetlands under varying conditions and is also applicable for global-scale simulations.

1 Introduction

Methane (CH_4) is an important greenhouse gas, with a 100-year global warming potential 28 times stronger than that of carbon dioxide (CO_2) (Myhre et al., 2013). Atmospheric CH_4 concentration in 2011 is 150 % greater than before 1750 (Hartmann et al., 2013). Wetlands, as an important component of the terrestrial ecosystem, play a vital role in the global carbon cycle, which includes a CH_4 budget (Zhang et al., 2002; Ciais et al., 2013). CH_4 emissions from natural wetlands are the main drivers of the global interannual variability of CH_4 emissions with high confidence and contribute largely to interannual variations and anomalies of atmospheric CH_4 concentrations (Ciais et al., 2013). Therefore, it is vital to improve existing CH_4 emission quantification methods for wetlands to better understand the global CH_4 budget (Chen et al., 2013; Kirschke et al., 2013; Nisbet et al., 2014).

Over the last decades, three approaches have generally been used in estimating CH_4 emissions from wetlands across different scales: (1) an extrapolation of flux measurements approach, which uses actual CH_4 emission measurements to calculate a global estimation, (2) a bottom-up approach, which uses process-based models to calculate CH_4 fluxes based on understanding of CH_4 emissions and their environmental controls, and (3) a top-down approach, which uses inverse models to estimate the distribution of CH_4 sources and sinks by incorporating atmospheric observations (e.g. satellite observations), an atmospheric transport model and prior estimates of source distributions and magnitudes (Arneth et al., 2010; EPA, 2010; Kirschke et al., 2013). The first approach can be unreliable in scaling from point measurements up to regional or global scales due to limitations in spatial and temporal coverage of measurements (Cao et al., 1996).

The currently used top-down approach – generally believed proficient in covering large regions – may inadvertently include some incomplete observations and error amplifications during inverse modelling processes (Chen and Prinn, 2005; Ciais et al., 2013). Process-based models can be used to improve CH_4 emission estimation under different climatic regimes and at the same time cope with the complex interactions that take place between soil, vegetation, and hydrology under CH_4 production and consumption processes. The development and application of process-based models could be a practical alternative approach when extrapolating results from site scale to regional or global scale (Cao et al., 1996; Li, 2000; Zhang et al., 2002).

Several process-based models have been developed to estimate global CH_4 emissions. Each has its own strategy and features to deal with wetland system complexity and CH_4 flux processes (Li, 2000; Walter and Heimann, 2000; Zhuang et al., 2004; Meng et al., 2012). Cao et al. (1995, 1996) developed a CH_4 emission model for rice paddies based on C substrate level, soil organic matter (SOM) degradation and environmental control factors and improved it for global natural wetland simulation; but the model has no specific CH_4 emission process. Walter and Heimann (2000) and Walter et al. (2001a, b) developed a 1-D process-based climate-sensitive model to estimate global long-term CH_4 emissions from natural wetlands, forced with net primary production derived by a separate model. Li (2000) developed a denitrification–decomposition model (DNDC) to simulate CH_4 emissions but only for rice paddies. Zhang et al. (2002) adopted the DNDC model and some of its key components to simulate wetland ecosystem emissions. Zhuang et al. (2004) have considered the important freeze–thaw processes and integrated methanogenesis modules into the Terrestrial Ecosystem Model (TEM), but only applied it to estimate net CH_4 emissions in the high-latitude area of the Northern Hemisphere. A process model (PEATLAND) was developed to simulate CH_4 flux from peat soils (van Huissteden et al., 2006) and up-scaled for global boreal and Arctic wetland simulations (Petrescu et al., 2010), although the model did not include explicit soil biogeochemical processes. Wania et al. (2010) integrated a CH_4 emission module into the modified dynamic global vegetation model Lund-Potsdam-Jena (LPJ) to simulate CH_4 emissions from northern peatlands with consideration of permafrost dynamics, peatland hydrology and peatland vegetation. This model was then modified to simulate global net CH_4 emissions for northern peatlands, naturally inundated wetlands and rice agriculture soils (Spahni et al., 2011). To characterize uncertainties and feedbacks between CH_4 flux and climate, Riley et al. (2011) developed a CH_4 biogeochemistry model (CLM4Me) and integrated it into the land component of the Community Earth System Model (CESM) and further analyses were conducted by Meng et al. (2012), but specific plant functional types have not been considered in wetlands.

The Wetland and Wetland CH_4 Inter-comparison of Models Project (WETCHIMP), which simulates and compares large-scale wetland characteristics and corresponding CH_4 emissions, reported that large uncertainties indeed still exist when estimating CH_4 emissions (Melton et al., 2013; Wania et al., 2013). These uncertainties are generally introduced from large temporal and spatial variations in CH_4 flux, with the complex processes that underlie CH_4 emissions and also the limited inherent range of field and laboratory measurements (Arneth et al., 2010; Wania et al., 2010; Spahni et al., 2011; Meng et al., 2012). Therefore, further development of process-based CH_4 emission models is critical (Walter and Heimann, 2000; Ito and Inatomi, 2012). A dynamic global vegetation model (DGVM) generally combines vegetation dynamics, biogeochemistry, and biogeography processes to predict terrestrial ecosystem response to rapid climate change (Prentice et al., 1989; Cramer et al., 2001). Integrating the CH_4 emissions module into a DGVM would be an efficient approach to reflect interactions between hydrology, vegetation, soil and CH_4-related processes, and subsequently reducing uncertainties in CH_4 emission estimation at different spatial and temporal scales (Arneth et al., 2010; Tian et al., 2010; Wania et al., 2010). It would also be a practical approach to apply when predicting spatial and temporal patterns of CH_4 emissions under different future climate change scenarios (Gedney et al., 2004; Shindell et al., 2004; Tian et al., 2010; Stocker et al., 2013). To date, only a few DGVM models have an integrated CH_4 emission module (Wania et al., 2010; Spahni et al., 2011).

Therefore, a new model development framework of TRIPLEX-GHG in which a CH_4 emission model based on a synthesis of the previous studies discussed was integrated into a DGVM of the Integrated Biosphere Simulator (IBIS). The IBIS is designed to integrate a variety of terrestrial ecosystem functions within a physically consistent modelling framework and represents land surface processes, canopy physiology, vegetation phenology, long-term vegetation dynamics and carbon exchange (Foley et al., 1996; Kucharik et al., 2000). In addition, a water table simulation module based on the approach developed by Granberg et al. (1999) was also integrated into the IBIS and a new plant function type for wetland was added as well. The objectives of the current study are to: (1) integrate biogeochemical-based methanogenesis processes into a DGVM, which includes explicit description of the processes of CH_4 production, oxidation and transportation, for the interactions between hydrology (e.g. water table), vegetation (e.g. specific plant function type in wetlands, primary production) and soil biogeochemistry; (2) make the model applicable throughout global natural wetlands by adjusting a few sensitive parameters.

2 Model description and key processes

The TRIPLEX-GHG model (Peng et al., 2013) is based on the legacy of well-established and published models that include IBIS (Foley et al., 1996), DNDC (Li, 2000), TRIPLEX (Peng et al., 2002) and CASACNP (Wang et al., 2010). However, the scope of this study was only to introduce the development of the new wetland water table and the methanogenesis modules. The basic concept and structure of CH_4 emission and water table models and their integration into the IBIS are presented in Fig. 1 and details are described below.

IBIS represents vegetation with plant functional types (PFTs) characterized in terms of biomass and leaf area index (LAI) to simulate changes in vegetation structure on an annual time step through PFT sunlight and water competition (Foley et al., 1996; Kucharik et al., 2000, 2006). For wetland simulations, a new PFT was added in the model. Most of the PFT phenological and physiological parameters were adopted from the C3 grass PFT in the original IBIS model. The definition of inundation stress effects on gross primary productivity (GPP) of the added PFT in wetlands followed the assumption made by Wania et al. (2009a), that sphagnum and C3 graminoids photosynthesis will increase or decrease when water table rises or drops.

2.1 Water table module

Since the water table is an essential factor in determining anoxic and oxic soil zone extent where CH_4 is produced and oxidized, respectively, a water table simulation module was integrated into the IBIS. The module primarily follows the approach developed by Granberg et al. (1999) and the approach has been applied to studies by Zhuang et al. (2004), Weiss et al. (2006) and Wania et al. (2009b). Although applications of the water table simulation approach by Granberg et al. (1999) have been primarily carried out for peatlands or mires, the method was extended for water table simulations of natural wetlands in addition to peatlands for this study. Water balance is the basis of water table simulations. Two zones separated by water table surface were specified for wetlands: the anoxic zone (saturated zone) and the oxic zone (unsaturated zone). Positioning of the water table is subject to soil moisture change, i.e. the input and output volume of water in a specific location. The assumption is that standing water can occur above the land surface and that the drainage process through the bottom of the soil layers can be omitted. When the position of water table is higher than maximum standing water, excess water will be released as runoff. The water budget in the wetland soil profile was derived from the deficit of water input (precipitation) and water output (evapotranspiration and runoff). The water table is estimated by the equation provided below, which was also described in the studies of Granberg et al. (1999) and Wania et al. (2009b):

$$\text{Water\_Table} = \begin{cases} V_{\text{tot}} - Z_{\text{acro}}\phi & \text{if WT} > 0 \\ -\sqrt{\frac{3.0\cdot(Z_{\text{acro}}\phi - V_{\text{tot}})}{2.0\cdot A_z}} & \text{if WT} \le Z_{\theta_{\text{s,min}}} \\ -\frac{3.0\cdot(Z_{\text{acro}}\phi - V_{\text{tot}})}{2.0\cdot(\phi - \theta_{\text{s,min}})} & \text{if WT} > Z_{\theta_{\text{s,min}}}, \end{cases} \quad (1)$$

where V_{tot} is total water content in the soil profile (cm), Z_{acro} is the maximum water table depth (30 cm, Frolking and Crill, 1994; Granberg et al., 1999; Zhuang et al., 2004), ϕ is the soil porosity (fraction), $\theta_{\text{s,min}}$ is the minimum volumetric water content at the soil surface (0.25, Granberg et al., 1999), $Z_{\theta_{\text{s,min}}}$ is the maximum depth where evaporation influences soil moisture (10 cm, Granberg et al., 1999). A_z is the gradient in the linearly decreasing interval, calculated as $A_z = (\phi - \theta_{\text{s,min}})/Z_{\theta_{\text{s,min}}}$. A negative/positive value of the water table indicates that the water table is below/above the soil surface, respectively.

2.2 Methane module

The CH_4 emissions module was adapted and integrated from a number of studies and models (Li, 2000; Walter and Heimann, 2000; Zhang et al., 2002; Wania et al., 2010; Riley et al., 2011; Spahni et al., 2011). Three major processes that include CH_4 production, transport (ebullition, diffusion, and plant-mediated transport) and oxidation were coupled with the IBIS. CH_4 is produced in each soil layer when soil conditions are favourable. The soil layers is 6 and the soil depth is set to 4 m as in the original IBIS model. The thermal and water balance processes were inherited from IBIS model. For the wetlands methane module, to simulate the dynamics of the water table, we divided the soil profile into 30 layers (1 cm per layer) above the maximum water table depth (30 cm). Thus 30 layers were used to simulate the water table changes and methane emission process. The soil above maximum water table depth was separated into anoxic and oxic zones, where CH_4 is produced and oxidized, respectively. The change in CH_4 for each time step in each soil layer is determined by the CH_4 production magnitude (Pro_{CH_4}), oxidation (Oxi_{CH_4}), and three transportation pathways (Ebullition: Ebu_{CH_4}, Diffusion: Dif_{CH_4}, and Plant Mediated Transport: PMT_{CH_4}). For each soil layer, CH_4 flux is the difference between production (Pro_{CH_4}) and consumption/emission ($\text{Pro}_{\text{CH}_4} - \text{Oxi}_{\text{CH}_4} - \text{Ebu}_{\text{CH}_4} - \text{Dif}_{\text{CH}_4} - \text{PMT}_{\text{CH}_4}$). Total CH_4 released to the atmosphere is the sum of the three-way transportation ($\text{Ebu}_{\text{CH}_4} + \text{Dif}_{\text{CH}_4} + \text{PMT}_{\text{CH}_4}$) of the total soil profile.

2.2.1 Methane production

CH_4 production is considered as the final stage of organic matter mineralization under anaerobic conditions (Cao et al., 1996). It depends not only on carbon substrate supply from plant primary production, but also on soil heterotrophic respiration rates and soil environmental conditions (such as the water table, soil temperature and hydrological regimes which

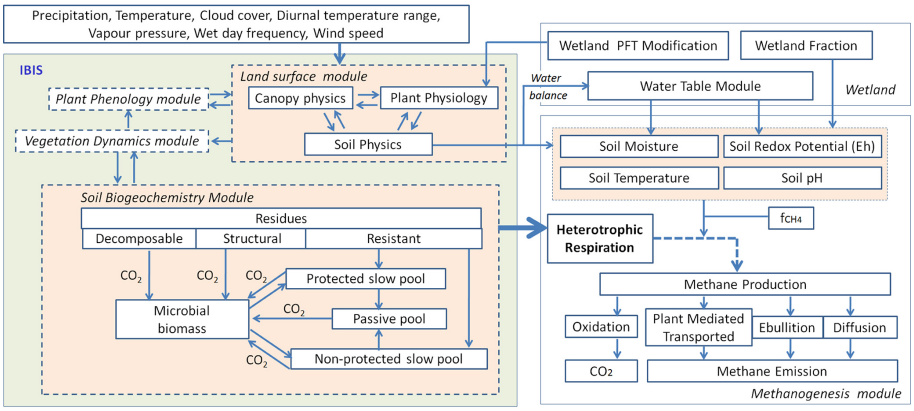

Figure 1. Basic structural concept and integration of CH_4 emission and the water table modules into DGVM of IBIS in TRIPLEX-GHG.

define the essential anaerobic conditions for methanogenesis) (Moore and Knowles, 1990; Sass et al., 1990; Whiting and Chanton, 1993; Cao et al., 1996; Walter and Heimann, 2000; Walter et al., 2001b).

CH_4 production was calculated as a proportion of heterotrophic respiration (CO_2–C) along with soil temperature, Eh and pH modification factors as follows:

$$\mathrm{Pro}_{CH_4} = R_H \cdot r \cdot f_{STP} \cdot f_{pH} \cdot f_{EhP}, \quad (2)$$

where R_H is the soil heterotrophic respiration rate ($gC\,m^{-2}\,day^{-1}$), calculated as the change in soil carbon pool size for each time step by the biogeochemical module in the IBIS. Along with the decomposition processes, carbon flows between different pools including above-ground and below-ground litter pools, a microbial pool, protected and nonprotected pools, and a passive pool. The carbon in litter and soil organic matter is partitioned between microbial biomass and respiration in decomposition processes, with assigned microbial efficiencies for each transformation among pools (Kucharik et al., 2000). A nitrogen feedback is added to control both above-ground carbon assimilation and below-ground soil organic carbon decomposition (Liu et al., 2005). f_{STP}, f_{pH} and f_{EhP} represent CH_4 production factors of soil temperature, pH and redox potential, respectively. r is the release ratio of CH_4 to CO_2.

Many studies have shown that CH_4 production is smaller or significantly lower than that found during growing seasons when soil temperature is below 0° C (Whalen and Reeburgh, 1992; Shannon and White, 1994). CH_4 emissions during winter are suggested to be produced during the previous growing seasons and stored in the soil profile (Dise, 1992; Melloh and Crill, 1996). Therefore, CH_4 production was only permitted in the module when soil temperature was above the freezing point (0° C) and below an extremely high temperature limit (45° C in this study). The relationship between soil temperature and CH_4 production was adapted from Zhang et al. (2002) as described below:

$$f_{STP} = \begin{cases} 0 \quad \text{if} \quad T_{soil} < 0 \\ 0 \quad \text{if} \quad T_{soil} > T_{max} \\ vt^{xt} \cdot \exp(xt \cdot (1 - vt)) \quad \text{if } 0 \le T_{soil} \le T_{max}, \end{cases} \quad (3)$$

where

$$vt = \left(\frac{T_{max} - T_{soil}}{T_{max} - T_{opt}}\right) \quad (4)$$

$$xt = \left[\log(Q_{10}) \cdot (T_{max} - T_{opt})\right]^2 \times \frac{\left[1.0 + \left(1.0 + 40.0/[\log(Q_{10}) \cdot (T_{max} - T_{opt})]\right)^{1/2}\right]^2}{400} \quad (5)$$

and T_{max} and T_{opt} are the highest temperature and optimum temperature for CH_4 production with values of 45 °C and 25 °C, respectively. T_{soil} is soil temperature (°C). For this study, a base Q_{10} value of 3.0 was used (Zhang et al., 2002) for simulations at different calibration sites.

Soil pH affected methanogenesis with a tolerance range between 5.5 and 9.0 while optimal values ranged between 6.4 and 7.8 with peak values ranging between 6.9 and 7.1 (Wang et al., 1993; Cao et al., 1995). Walter and Heimann (2000) included the effects of pH on CH_4 production in the tuning parameter. The approach by Cao et al. (1995) was adopted here to express the relationship between soil pH and CH_4 production:

$$f_{pH} = \begin{cases} 0 \quad \text{if } pH_{soil} > pH_{high} \text{ or } pH_{soil} < pH_{low} \\ \left(\frac{pH_{soil} - pH_{low}}{pH_{opt} - pH_{low}}\right) \cdot \left(\frac{pH_{high} - pH_{soil}}{pH_{high} - pH_{opt}}\right)^{\frac{pH_{high} - pH_{opt}}{pH_{opt} - pH_{low}}} \end{cases} \quad (6)$$

where pH_{low} and pH_{high} represent low (4.0) and high (9.0) limitations of pH effect intervals. The optimal value was set at 7.0. Soil pH is taken from the soil properties data set.

Inundation causes low redox potential and promotes an anaerobic soil environment that will stimulate methanogenesis. The soil layer is considered to be inundated below the water table surface and the inundated condition of each soil layer changes with the dynamics of the water table. A linear relationship between soil water table position and CH_4 production was previously used to represent the effects of redox potential (Cao et al., 1996). In this study, redox potential changes are determined by water table position, water-filled pore space (WFPS) fraction, as well as root distribution (Zhang et al., 2002; Zhuang et al., 2004). For the effects of redox potential on methanogenesis, Cao et al. (1995) applied a switch value (−200 mV) for CH_4 production processes, while Li (2000) assumed that CH_4 production takes place with a soil Eh level below −150 mV. The relationship between redox potential and CH_4 production used in this study was generalized by Zhang et al. (2002), based on the studies by Fiedler and Sommer (2000) and Segers (1998). When redox potential is within a range between −200 mV and −100 mV, its effect on methanogenesis diminishes linearly from 1.0 to 0.0. Otherwise, the factor is equal to 1.0 and 0.0 when redox potential is less than −200 mV and greater than −100 mV, respectively.

The assumption in calculation of the parameter r in the CH_4 production adopted here was used in the CLM4Me (Riley et al., 2011; Meng et al., 2012) and LPJ-WHyMe (Wania et al., 2010; Spahni et al., 2011) models, in which CH_4 production within the anaerobic portion of the soil column relates to soil heterotrophic respiration, and where the soil carbon for methanogenesis is considered as a fraction of soil heterotrophic respiration.

2.2.2 Methane oxidation

CH_4 is oxidized by aerobic methanotrophic activities in the soil, taking place in the unsaturated zone above the water table (Cao et al., 1996; Li, 2000; Zhuang et al., 2004). The rate of CH_4 oxidation can be calculated based on a linear relationship with GPP (Cao et al., 1996) or as a function of soil CH_4 concentration and Eh (Li, 2000). Given that CH_4 oxidation is primarily controlled by CH_4 concentration, redox potential and soil temperature (Segers, 1998), the equation used here is as follows:

$$\mathrm{Oxi}_{\mathrm{CH_4}} = A_{\mathrm{CH_4}} \cdot f_{\mathrm{CH_4}} \cdot f_{\mathrm{STO}} \cdot f_{\mathrm{EhO}}, \quad (7)$$

$A_{\mathrm{CH_4}}$ is the amount of CH_4 in each soil layer ($\mathrm{gC\,m^{-2}\,layer^{-1}}$). The CH_4 concentration factor ($f_{\mathrm{CH_4}}$) is represented by a Michaelis–Menten kinetic relationship: $C_{\mathrm{CH_4}}/(K_{\mathrm{CH_4}} + C_{\mathrm{CH_4}})$, where $C_{\mathrm{CH_4}}$ is the CH_4 concentration ($\mu\mathrm{mol\,L^{-1}}$) and $K_{\mathrm{CH_4}}$ is the half-saturation coefficient with respect to CH_4 and set to $5\,\mu\mathrm{mol\,L^{-1}}$ (Walter and Heimann, 2000; Zhang et al., 2002; Riley et al., 2011). A Q_{10} value of 2.0 based on results from previous studies (Segers, 1998; Walter and Heimann, 2000; Zhang et al., 2002) was used to quantify soil temperature effects on CH_4 oxidation (f_{STO}). The term for redox potential effects on CH_4 oxidation (f_{EhO}) was adopted from a general relationship between redox potential and CH_4 oxidation reported by Zhang et al. (2002), which was taken from Fiedler and Sommer (2000) and Segers (1998). The redox potential factor was set to zero and 1.0 when Eh was below −200 mV and above 200 mV, respectively. In the remaining range of −200 to −100 mV and −100 to 200 mV, the effective factors of redox potential were represented by two simple linear functions, varying from 0 to 0.75 and from 0.75 to 1, respectively.

2.2.3 Methane emission processes

In early studies, no specific CH_4 emission process in CH_4 modelling existed (Cao et al., 1995, 1996). Generally, major CH_4 emission processes, including diffusion, ebullition and plant-mediated transportation, were formulated by the release of more recent models (Li, 2000; Walter and Heimann, 2000; Wania et al., 2010; Riley et al., 2011), as have been considered in this study.

CH_4 diffusion between soil layers was estimated here using Fick's law based on the CH_4 concentration gradient in the soil profile (Walter and Heimann, 2000; Zhuang et al., 2004). The diffusion coefficient for each soil layer was modelled as follows:

$$D_i = D_{\mathrm{a}} \cdot f_{\mathrm{coarse}} \cdot f_{\mathrm{tort}} \cdot \mathrm{SoilPoro} \cdot (1 - \mathrm{WFPS}_i) + D_{\mathrm{w}} \cdot \mathrm{WFPS}_i, \quad (8)$$

where D_{a} and D_{w} are the CH_4 molecular diffusion coefficients in air with a value of $0.2\,\mathrm{cm^2\,s^{-1}}$ and in water with a value of $0.00002\,\mathrm{cm^2\,s^{-1}}$, respectively (Walter and Heimann, 2000). D_{a} and D_{w} reflect differences in the rate of CH_4 molecular diffusion through unsaturated versus saturated soil layers. f_{coarse} is the relative volume of coarse pores depending on soil texture (fraction) (Zhuang et al., 2004). f_{tort} is the tortuosity coefficient with a value of 0.66 (Walter and Heimann, 2000). Lastly, SoilPoro is soil porosity and WFPS is the water-filled pore space.

Being a relatively rapid channel for CH_4 emissions, bubbles will form as soon as CH_4 concentrations in the soil profile exceed a certain threshold (Walter and Heimann, 2000). For CH_4 ebullition emission processes, a constant threshold value of $750\,\mu\mathrm{mol\,L^{-1}}$ (Walter and Heimann, 2000; Zhang et al., 2002) was used in this study.

Vascular plants provide an effective pathway for CH_4 transport to the atmosphere (Shannon et al., 1996; Walter and Heimann, 2000). The plant-mediated flux is proportional to CH_4 concentration in the soil and is related to the concentration gradient between the soil and the atmosphere (Walter and Heimann, 2000). A simple equation was used to describe plant-mediated emissions based on the plant aerenchyma factor:

$$\mathrm{PMT}_{\mathrm{CH_4}} = f_{\mathrm{rhi}} \cdot f_{\mathrm{aer}} \cdot \mathrm{CH_{4gra}}, \quad (9)$$

where f_{rhi} is the rhizospheric oxidation factor, suggesting that a relatively large proportion of CH_4 will be oxidized in the highly oxic rhizospheric zone before entering plant tissue (Wania et al., 2010). The factor is dependent on plant type and can range between 20 % and 100 % (Strom et al., 2005; Wania et al., 2010) and a constant value of 0.5 was used here (Zhang et al., 2002). f_{aer} is the plant aerenchyma factor estimated as a function of root length density (converted from root biomass using a specific root length of 2.1 cm mg^{-1}), the area of the cross section of a typical fine root (assumed as a constant of 0.0013 cm^2) and the degree of gas diffusion from root to atmosphere (a scalar determined by the aerenchyma condition of plants) (Zhang et al., 2002). A simplified constant of 0.5 was used as the degree of gas diffusion from root to atmosphere in this study, since the value should be 1 for the plants with well-developed aerenchyma (e.g. grasses and sedges) and be 0 for the plants without aerenchyma (e.g. sphagnum and moss). CH_{4gra} is the CH_4 deficit between the soil profile and the atmosphere (gC m^{-2} $layer^{-1}$).

2.2.4 Major parameters in methane module

The major parameters for the CH_4 module are presented in Table 1. Some of the parameters adopted values that have been fully discussed and supported in previous studies (Cao et al., 1996; Segers, 1998; Walter and Heimann, 2000; Zhang et al., 2002; Zhuang et al., 2004; Wania et al., 2010; Meng et al., 2012).

3 Data and method

3.1 Study sites

Observed CH_4 emissions data of natural wetlands based on previous studies or field work (19 sites worldwide from 35 studies) were collected for model sensitivity analysis, parameter fitting and calibration. Information related to these wetland sites, including location, wetland type, measurement method and references are summarized in Table 2. The selected sites have a wider geographical spread over low- to mid- to high-latitude regions.

Many of the sites listed in Table 2 have been also used in other CH_4 emission modelling tests. Since there were no observed detailed individual plot data in the studies carried out in the Amazon Basin (Bartlett et al., 1988, 1990; Devol et al., 1988; Melack et al., 2004) and South Florida (Burke Jr. et al., 1988; Harriss et al., 1988), with only observed emission rate throughout the regions, region-based average emission rates were compared between prediction and estimation. For some sites where different studies were carried out by different groups in the same or different time period (e.g. Sanjiang plain, Stordalen, Minnesota, Table 2), comparisons were made between the same modelling results and those results from different studies. Observation period modelling results were used for parameter fitting and model performance evaluation. Monthly and yearly emission rates were calculated from simulated daily rates when comparing with monthly and yearly observed data.

3.2 Input data

For the regional simulations conducted in the Amazon Basin and South Florida, the CRU-TS 3.1 Climate Database (http://badc.nerc.ac.uk/data/cru) was adopted to construct monthly climate input data for the two regions. Selected variables include cloud cover, diurnal temperature range, precipitation, temperature, vapour pressure and wet-day frequency. For the site-based simulations in China, daily climate data were obtained from the Meteorological Bureau of China. For the other sites, since directly measured climate data was unavailable, the daily climate data (mean, max, min temperature, precipitation, mean wind speed, dew point) were downloaded from the nearest stations to the evaluation sites in the global data set of Global Summary of the Day (GSOD) (http://www7.ncdc.noaa.gov/CDO/cdoselect.cmd?datasetabbv=GSOD&countryabbv=&georegionabbv=) to drive the model. Being unavailable in GSOD, the station-based cloud cover data are extracted from the CRU-TS data set for each evaluation site. Climate data used for the model spin-up period were mean observed data for site-based simulation or 30-year (1961–1990) means of the CRU data (http://www.ipcc-data.org/obs/get_30yr_means.html) for regional simulation in Florida and the Amazon Basin.

CO_2 concentration data for the simulation period were composed of two parts. Observed CO_2 concentrations were used for the period covering 1958–2009, derived by Keeling et al. (2005) from in situ air measurements taken at Mauna Loa Observatory, Hawaii. CO_2 concentrations before 1958 were adopted from the IS92a global CO_2 concentration yearly data set, derived using a spline fit of Mauna Loa and ice core data (Enting et al., 1994).

The soil classification map used was based on the Digital Soil Map of the World (DSMW), generated from the FAO-UNESCO Soil Map of the World (http://www.fao.org/geonetwork/srv/en/metadata.show?id=14116). DSMW attributes were connected with the soil properties data set contributed by Batjes (2006) that describes characteristics of soil texture (soil clay, sand and silt fraction) and soil pH. A global soil data set (IGBP-DIS, 2000) was adopted to generate soil carbon data for model initialization.

A global digital elevation model (DEM) with an approximate 1 km spatial resolution (GTOPO30) was used for the topographic input data.

3.3 Initial sensitivity analysis for parameters fitting

For the model parameter fitting, initial sensitivity analysis experiments were conducted to obtain the most sensitive parameters in order to simplify the fitting processes.

Table 1. List of major parameters in CH_4 production, oxidation and transportation.

Process	Parameters	Values	Unit	Description	References
Methane production	T_{max}	45	°C	highest temperature for methane production	This study
	T_{opt}	25	°C	optimum temperature for methane production	This study
	pH_{high}	9	–	highest pH for methane production	Cao et al. (1996), Zhang et al. (2002), Zhuang et al. (2004)
	pH_{low}	4	–	lowest pH for methane production	Cao et al. (1996), Zhang et al. (2002), Zhuang et al. (2004)
	pH_{opt}	7	–	optimum pH for methane production	Cao et al. (1996), Zhang et al. (2002), Zhuang et al. (2004)
	r	0.1–0.4	–	ratio of CH_4 and CO_2	Wania et al. (2010), Zhang et al. (2002)
	Q_{10}	1.7–16	–	Q_{10} for methane production	Dunfield et al. (1993), Walter and Heimann (2000)
Methane oxidation	K_{CH_4}	5	µmol	Michaelis–Menten coefficients	Walter and Heimann (2000), Zhang et al. (2002)
	Q_{10}	1.4–2.4	–	Q_{10} for methane oxidation	Meng et al. (2012), Walter and Heimann (2000), Zhang et al. (2002), Segers (1998)
Methane transport	f_{tort}	0.66	–	tortuosity coefficient	Walter and Heimann (2000)
	D_a	0.2	$cm^2\,s^{-1}$	molecular diffusion coefficient of methane in air	Walter and Heimann (2000)
	D_w	0.00002	$cm^2\,s^{-1}$	molecular diffusion coefficient of methane in water	Walter and Heimann (2000)
	f_{rhi}	0.5	–	factor of rhizospheric oxidation	Wania et al. (2010), Zhang et al. (2002)

Based on analyses carried out in previous studies, the Q_{10} (for processes of CH_4 production and oxidation) and the release ratio of CH_4 to CO_2 (r) were selected for initial sensitivity analysis for parameter fitting. Obtaining an optimal sensitive parameter combination at each individual site was then attempted. Previous studies have shown that CH_4 production and oxidation are primarily dependent on temperature, which is controlled by Q_{10} values (Cao et al., 1996; Walter and Heimann, 2000; Walter et al., 2001a; Riley et al., 2011). The Q_{10} values have large uncertainty with broad ranges (Dunfield et al., 1993; Westermann, 1993), which may be caused by substrate availability (Valentine et al., 1994), as well as the influence of temperature on plant growth and organic matter decomposition (Cao et al., 1996). Some studies have shown observed Q_{10} values ranging from 1.7 to 16 (Dunfield et al., 1993; Valentine et al., 1994) or from 1.7 to 4.7 (Valentine et al., 1994). Cao et al. (1996) used a Q_{10} value of 2.0 while Walter and Heimann (2000) and Walter et al. (2001b) used a Q_{10} value of 6.0. Zhuang et al. (2004) used an ecosystem-specific Q_{10} coefficient to evaluate soil temperature effects on CH_4 production at northern high latitudes. The parameter r in the CH_4 production was considered as the most important and influencing parameter for CH_4 emissions (Wania et al., 2010; Spahni et al., 2011). Cao et al. (1995, 1996) used a constant ratio to represent the proportion of decomposed organic carbon that can be converted to CH_4. Walter and Heimann (2000) and Walter et al. (2001b) used a tuning parameter calculated using a simple multiple linear regression of soil organic carbon and mean annual temperature to adjust the amplitude of simulated CH_4 emissions. Zhuang et al. (2004) used an ecosystem-specific potential rate for CH_4 production.

Sensitivity is generally expressed as the ratio between a relative change of model output and a relative change of a parameter. The sensitivity index described in Lenhart et al. (2002) was used to quantify sensitivity in this study. The sensitivity index (I) is expressed as a finite difference in approximation of a partial derivative, which indicates the dependence of a variable (y) from a parameter (x):

$$I = \frac{(y_2 - y_1)/y_0}{2\Delta x / x_0}, \tag{10}$$

where y_0 is the model output with an initial parameter of x_0. The initial parameter value varied by $\pm\Delta x$ ($x_1 = x_0 - \Delta x$ and $x_2 = x_0 + \Delta x$) with corresponding values y_1 and y_2. The sign of sensitivity index (I) indicates the direction of the model's reaction to parameter change. According to Lenhart et al. (2002), calculated sensitivity indices are ranked into four classes (small to negligible, medium, high, very high). Model sensitivity to a specific parameter is small to negligible when the absolute value of the sensitivity index is less than 0.05 but very high when the absolute value of the sensitivity index is greater than or equal to 1.0.

3.4 Methods for parameter fitting evaluation

After the initial sensitivity analysis, parameter fitting processes for the selected most sensitive parameters was conducted to find the best combination of site-specific parameters. Indices including root mean square error (RMSE), coefficient of determination (R^2) and index of agreement (D)

Table 2. Information of collected sites for model parameter fitting. The information of nearest GSOD station for each site appended.

ID	Sites	Location	Lat	Long	Type	Biome	Time	Method	Reference	GSOD station ID	GSOD station name
1	Stordalen	Sweden	68°20′ N	19°03′ E	subarctic mire	Boreal	1974/1994/1995	static chamber	Svensson et al. (1999)	020200	Katterjakk
							2006–2007	automatic chamber	Jackowicz-Korczynski et al. (2010)		
2	Degero Stormyr	Sweden	64°11′ N	19°33′ E	boreal mire, fen	Boreal	1995–1997	static chamber	Grandberg et al. (2001)	022740, 022860	Vindeln, Umea
3	Salmisuo mire	Finland	62°47′ N	30°56′ E	boreal fen	Boreal	1993	static chamber	Saarnio et al. (1997)	029290	Joensuu
4	Ruovesi	Finland	61°50′ N	24°12′ E	boreal fen	Boreal	2005	eddy covariance technique	Rinne et al. (2007)	029450	Halli
5	Plotnikovo West Siberia	Russia	57°00′ N	82°00′ E	ombrotrophic bogs	Boreal	Jul 1993–1997	static chamber	Panikov and Dedysh (2000)	293280, 296310	Bakchar, Kolyvan
6	Fairbanks Alaska	USA	64°48′ N	147° 42′ W	wetland	Boreal	1987–1990	static chamber	Ojima et al. (1992)	702610	Fairbanks Intl Arpt
7	BOREAS SSA	Canada	53°48′ N	104° 37′ W	peatland, fen	Boreal	1994–1995	eddy covariance technique & static chamber	Sellers et al. (1997)	718690	Prince Albert Arpt
8	BOREAS NSA	Canada	55°55′ N	98°25′ W	peatland, fen	Boreal	1994/1996	static chamber	Sellers et al. (1997)	710790	Thompson Airport
9	Quebec	Canada	53°54′ N	78°46′ W	peatland	Boreal	2003	static chamber	Pelletier et al. (2007)	716278	Kuujjuarapik Arpt
			53°38′ N	77°43′ W	peatland		2003	static chamber		718270	La Grande Riviere
			53°34′ N	76°08′ W	peatland		2003	static chamber		718113	Nemiscau Arpt (Sawr)
10	Sanjiang plain	China	47°35′ N	133°31′ E	marshland	Temperate	2002–2005	open-bottom chamber	Huang et al. (2010)	–	–
					natural freshwater wetland		2002–2005	dark chamber and gas chromatography techniques	Song et al. (2009)		
					marshland		2001	static chamber	Wang et al. (2002b)		
					marshland		1995–1996	static chamber	Cui et al. (1997)		
					freshwater marsh		2001–2002	open-ended plexiglass chambers	Ding et al. (2004)		
					marshland		2003	static chamber	Yang et al. (2006)		
					marshland		2002	static chamber	Hao et al. (2004)		
11	Qinghai–Tibet	China	32°47′ N	102°32′ E	peatland	Temperate	2001	static chamber	Wang et al. (2002a)	–	–
					peatland		2001–2002	open-ended plexiglass chambers	Ding et al. (2004)		
		China	33°56′ N	102°52′ E	peatland		2005–2006	static chamber	Chen et al. (2008)		
12	Minnesota	USA	47°32′ N	93°28′ W	peatland	Temperate	1988–1990	static chamber	Dise (1993)	727450	Duluth Intl Airport
							1991–1992	eddy covariance technique & static chamber	Clement et al. (1995)		
13	Michigan	USA	42°27′ N	84°01′ W	peatland, buck hollow bog	Temperate	1991–1993	static chamber	Shannon and White (1994)	725395	Jackson Co Reynolds
14	Sallies Fen	USA	43°12.5′ N	71°3.5′ W	fen	Temperate	1994–2001	static chamber	Zhuang and Crill (2008)	726055	Pease Intl Tradepor
15	Loch Vale, Colorado	USA	40°17′ N	105°39′ W	subalpine wetland	Temperate	1996–1998	closed chamber	Wickland et al. (2001)	724675	Eagle Co Rgnl
16	Mer Bleue	Canada	45°41′ N	75°48′ W	peatland, bog	Temperate	2004–2007	static chamber	Moore et al. (2011)	710630	Ottawa Recreation C
17	Ryans 1 Billagong	Australia	36°07′ S	146°58′ E	freshwater wetland	Temperate	Apr 1993–May 1994	static chamber	Boon (1995)	948990	Corryong Parish Lan
18	Florida	UAS	25°00′ N	81°00′ W	everglade	Tropical	Jan–Feb, 1984; Dec, 1985	portable gas filter correlation (GFC) measurement system	Bartlett et al. (1989)	–	–
			South Florida		everglade		Jun, Nov 1986; Mar, Aug 1987	static chamber	Burke Jr. et al. (1988)		
			South Florida		everglade		1980; 1982; 1985	gas filter correlation infrared absorption analyzer integrated with an open bottom chamber	Harriss et al. (1988)		
19	Amazon	Brazil	Amazon Basin		flooded plain	Tropical	1979–1987	satellite inverse	Melack et al. (2004)	–	–
							Jul–Aug, 1985	static chamber	Devol et al. (1988)		
							18 Jul–2 Sep, 1985	static chamber and gas filter correlation	Bartlett et al. (1988)		
							Apr–May, 1987	static chamber and gas filter correlation	Bartlett et al. (1990)		

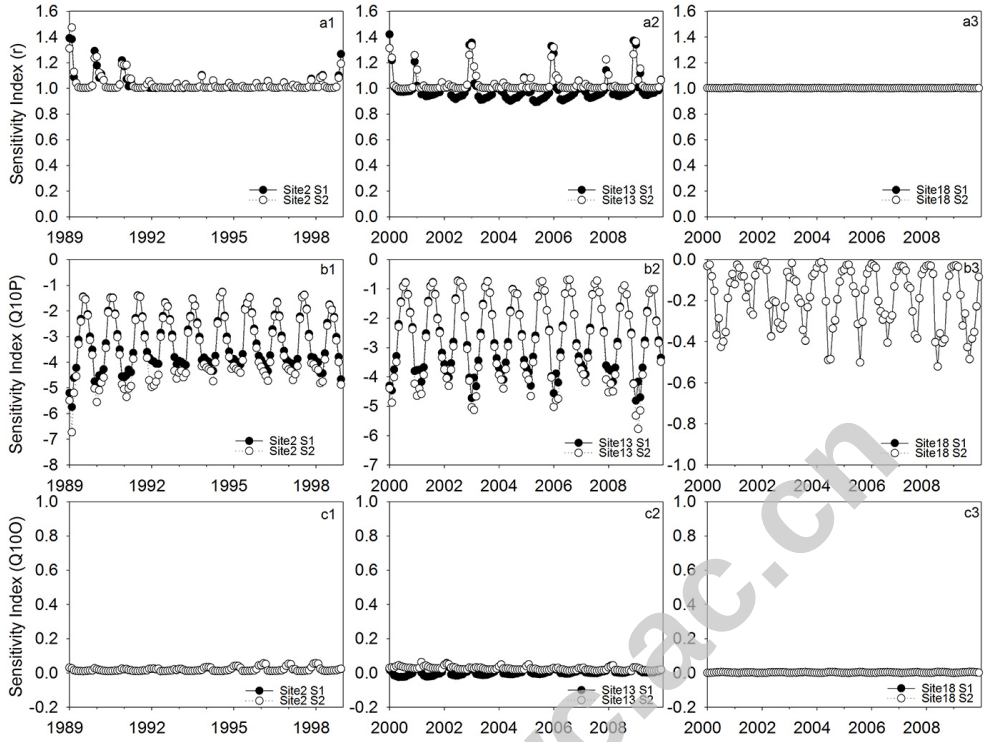

Figure 2. Sensitivity analysis of the three parameters (r, Q_{10}P, Q_{10}O) in the CH_4 module at three selected sites for different biome regions: boreal (site 2), temperate (site 12), and tropical (site 18). S1: scenario with single Δx; S2: scenario with double Δx.

were used to evaluate the model's performance. The RMSE was calculated as

$$\mathrm{RMSE} = \sqrt{\frac{\sum_{i=1}^{n}(S_i - O_i)^2}{n}}, \quad (11)$$

where S are the simulated and O the observed values; n is the number of data. The D is calculated as

$$D = 1 - \frac{\sum_{i=1}^{n}(S_i - O_i)^2}{\sum_{i=1}^{n}(|S_i - \overline{O}| + |O_i - \overline{O}|)^2}, \quad (12)$$

where $\overline{O}$ is the average of observed values. D varies between 0 and 1 and it is overly sensitive to extreme values (Willmott, 1981). A D value of 1 indicates a perfect match, and 0 indicates no agreement at all.

4 Results

4.1 Initial sensitivity analysis

Based on the initial values, Δx was set at 0.2 for Q_{10} in CH_4 production (Q_{10}P) and CH_4 oxidation (Q_{10}O), and set at 0.05 for the release ratio of CH_4 to CO_2 (r). Two scenarios were considered, with single Δx (S1) and double Δx (S2). The initial sensitivity tests were conducted at three sites (site 2, site 13 and site 18, Table 2) by the biome type (boreal, temperate and tropical regions).

Over different biomes, sensitivity analysis results indicate that r (Fig. 2a1–a3) and Q_{10}P (Fig. 2b1–b3) were very sensitive, while Q_{10}O had a very low model sensitivity with a sensitivity index (I) of less than 0.05 (Fig. 2c1–c3). Seasonal patterns of I show that the model was more sensitive to Q_{10}P during winter than other seasons in boreal (Fig. 2b1) and temperate (Fig. 2b2) regions. In contrast, the model was more sensitive during the summer than other seasons in the tropical region (Fig. 2b3). To simplify parameter fitting and make processes efficient as well as to assess model performance while reducing fluctuating parameters to as few as possible, Q_{10}O was set as a constant value (2.0) and only two adjustable parameters were chosen (r and Q_{10}P) during the parameter fitting discussed below.

4.2 Model parameterization and calibration

Calibration sites were categorized into three main biome regions: tropical, temperate and boreal (Table 2). Parameters r and Q_{10}P were adjusted to yield the best agreement for each site between simulation and observations (Figs. 3–5). The best parameter combination as well as the initial conditions of soil carbon and biomass after spin-up running for

Table 3. List of calibrated values for the parameters of r and Q_{10}P, the initial soil carbon and biomass conditions, and the model performance criteria indices for each site.

ID	Sites	r (CH_4 / CO_2)	Q_{10}P	Initial Soil Carbon (kgC m^{-2})	Initial Biomass(kgC m^{-2})	RMSE	R^2	D	Counts
1	Stordalen	0.13	2.00	17.12	1.36	0.03	0.67	0.83	17
2	Degero Stormyr	0.12	2.00	38.45	4.04	0.01	0.79	0.94	13
3	Salmisuo mire	0.27	1.70	31.23	5.77	0.04	0.55	0.83	6
4	Ruovesi	0.10	1.60	17.44	6.66	0.01	0.90	0.93	10
5	Plotnikovo West Siberia	0.20	2.00	24.00	6.19	0.09	0.52	0.73	6
6	Fairbanks Alaska	0.20	2.00	22.53	3.03	0.01	0.88	0.88	37
7	BOREAS SSA	0.22	2.00	27.46	6.08	0.06	0.54	0.85	12
8	BOREAS NSA	0.25	2.00	47.86	7.30	0.04	0.32	0.69	10
9	Quebec	0.10	3.00	20.91	4.69	0.02	0.93	0.94	9
10	Sanjiang plain	0.45	3.50	12.99	2.54	0.10	0.74	0.90	22
11	Qinghai–Tibet	0.21	3.00	31.57	3.45	0.07	0.54	0.76	20
12	Minnesota	0.14	2.30	13.07	8.30	0.03	0.70	0.91	44
13	Michigan	0.39	2.00	11.68	5.63	0.09	0.66	0.90	36
14	Sallies Fen	0.18	2.00	17.01	9.26	0.23	0.28	0.50	74
15	Loch Vale,Colorado	0.70	2.00	8.08	7.74	0.04	0.88	0.90	25
16	Mer Bleue	0.10	3.00	10.43	9.05	0.11	0.05	0.42	27
17	Ryans 1 Billagong	0.35	3.50	8.71	2.80	0.05	0.86	0.93	14
18	Florida	0.15	3.00	24.02	1.20	–	–	–	–
19	Amazon Basin	0.15	4.50	10.24	11.52	–	–	–	–

each site are listed in Table 3. The evaluation indices for the model performance were calculated with monthly results as also listed in Table 3. The release ratio of CH_4 to CO_2 ranged from 0.1 to 0.7 with a mean value of 0.23, and the Q_{10} value for CH_4 production ranged from 1.6 to 4.5 with a mean value of 2.48. Considering the different biome regions of boreal, temperate and tropical, parameter r has mean values of 0.18, 0.32, and 0.15, and parameter Q_{10}P has mean values of 2.03, 2.66, and 3.75, respectively.

4.2.1 Boreal region

Data on five natural European wetland sites located in the boreal region were collected, including one subarctic mire site and one boreal mire site in Sweden (Svensson et al., 1999; Granberg et al., 2001; Jackowicz-Korczyński et al., 2010), two boreal fen sites in Finland (Saarnio et al., 1997; Rinne et al., 2007) and one ombrotrophic bog site in Russia (Panikov and Dedysh, 2000).

Svensson et al. (1999) and Jackowicz-Korczyński et al. (2010) took CH_4 emission measurements at the same site during different time periods (Fig. 3a, b). The mean emission rate of four wet and semi-dried sites in Svensson et al.'s (1999) study and data observed with the automatic chamber system in Jackowicz-Korczyński et al.'s (2010) study were used for comparison (Fig. 3a, b). CH_4 emission rates ranged approximately from 0.02 to 4.9 gC m^{-2} month^{-1} in the study by Svensson et al. (1999) and approximately from 0.9 to 5.3 gC m^{-2} month^{-1} in the study by Jackowicz-Korczyński et al. (2010). It was difficult for the model to catch peak values for some years at this location (Fig. 3a, b). For another study (Granberg et al., 2001) carried out in a boreal mire in Sweden, however, the model simulated seasonal CH_4 emission variability with reasonable accuracy (RMSE = 0.01, $D = 0.94$, Fig. 3c).

We have compared modelled results from the current study with mean emission rates of four different vegetation surfaces (hummocks, flarks, *Eriophorum* lawns and *Carex* lawns) from a study by Saarnio et al. (1997) (Fig. 3d). Modelled daily CH_4 emission rates agreed reasonably with ranges of observed scatter points (RMSE = 0.04, $R^2 = 0.55$, $D = 0.83$) (Fig. 3d), while there was a time lag for the peak simulation.

A CH_4 flux study by Rinne et al. (2007) was measured using the eddy covariance technique. Gap-filling data using linear interpolation in that study was adapted for the modelling test carried out in the current study. Variation in modelled CH_4 emissions was consistent with that observed before early July and after mid-September (Fig. 3e). During the period from early July to mid-September, there was a drop in observed emission rates (Fig. 3e). Modelled emission rates showed higher values than observed emission rates during this period (Fig. 3e). Overall, emission rates agreed well between observation and simulation (RMSE = 0.01, $R^2 = 0.9$, $D = 0.93$).

In a study by Panikov and Dedysh (2000), annual variation in CH_4 emissions was relatively high, even during the same season. For example, emission rates in July ranged from 3.2 gC m^{-2} month^{-1} (1997) to 10.8 gC m^{-2} month^{-1} (1995) (Fig. 3f). The model simulated CH_4 emissions at this site reasonably well (RMSE = 0.09, $D = 0.73$) with the exception of those years that exhibited extremely high variation (e.g. 1993 and 1995) (Fig. 3f).

Figure 3g and h show the comparison of CH_4 emission rate between model simulations and observations obtained from the Boreal Ecosystem-Atmosphere Study

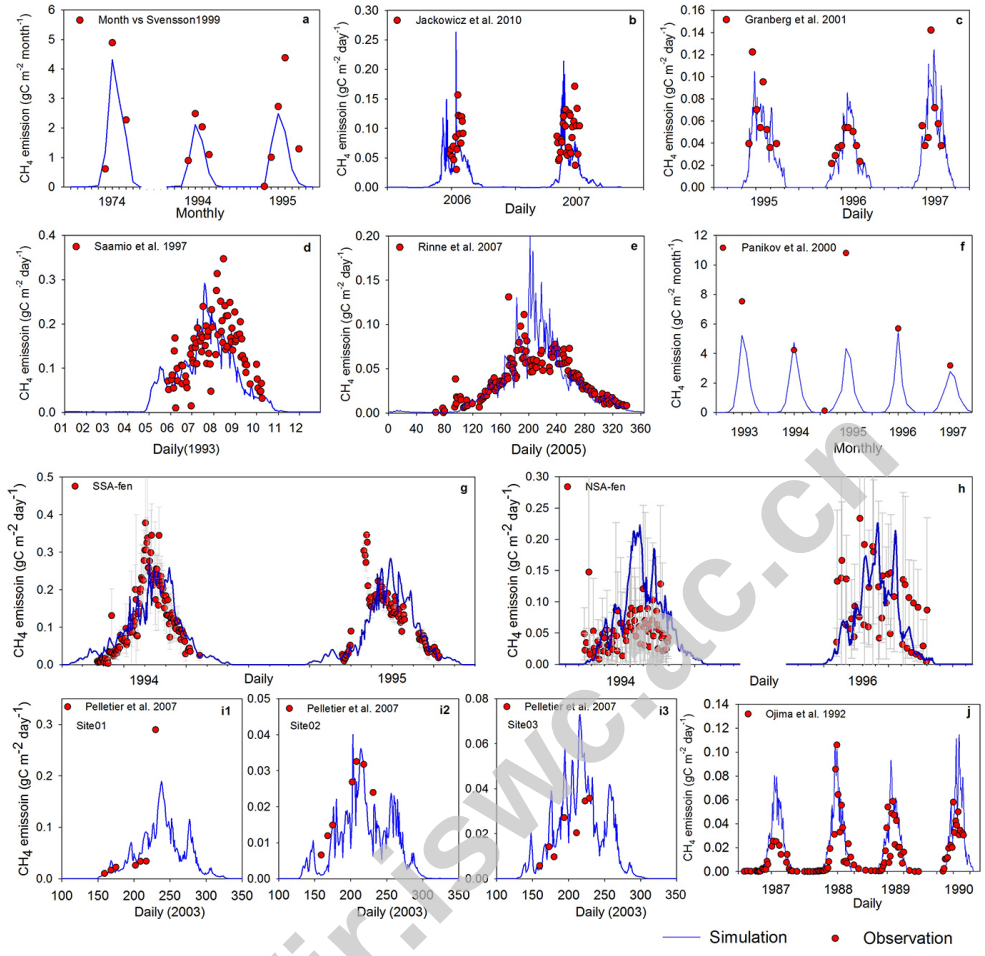

Figure 3. Comparison of modelled and observed CH_4 emissions for the sites located in the boreal region.

(BOREAS), a large-scale international interdisciplinary experiment situated in the northern boreal forests of Canada (Sellers et al., 1997). Daily observed CH_4 emission rates collected from the Southern Study Area (SSA-fen) and the Northern Study Area (NSA-fen) were used for comparison (http://daac.ornl.gov/BOREAS/bhs/BOREAS_Home.html). The magnitude of observed CH_4 emission rates for SSA was approximately twice that for NSA. For NSA, the mean CH_4 emission rate for 1996 was nearly twice that of 1994. These patterns indicate high temporal and spatial variation associated with CH_4 flux in these areas. The model had better performance in SSA ($R^2 = 0.54$, $D = 0.85$) than in NSA ($R^2 = 0.32$, $D = 0.69$). For SSA, the model failed to capture the 1994 peak emission. There was an approximate one month delay for the simulated peak emission rate when compared to observed data from 1995. For NSA, the model overestimated the 1994 CH_4 emissions while 1996 showed relatively better performance.

From a study by Pelletier et al. (2007), observed CH_4 emission rates measured on peatland covered by different vegetation types (excluding pools) was averaged for comparison. Based on the monthly mean emission rates comparison, the simulations agreed well with the observations (RMSE = 0.02, $R^2 = 0.93$, $D = 0.94$) (Fig. 3i1–i3).

Observational data of the Fairbanks site (Fig. 3j) was obtained from The United States Trace Gas Network (TRAGNET) online database (http://www.nrel.colostate.edu/projects/tragnet/) described in a workshop reported by Ojima et al. (1992). The model performed well (RMSE = 0.01, $R^2 = 0.88$, $D = 0.88$) except for some cases of overestimation during growing seasons.

4.2.2 Temperate region

Two sites in China were selected to test the model, one in northeast China and one in the Qinghai–Tibet Plateau. Natural wetlands and floodplains in China are primarily located in these two key regions (Ma et al., 2012). Figure 4a and b show comparisons between field measurements and model simulations in the Sanjiang Plain in northeast China. Figure 4a shows mean annual CH_4 emissions from wetlands of different plant types in a study by Huang et al. (2010) compared to

annual CH_4 emission rates of inundated marshes in a study by Song et al. (2009). CH_4 emission rates reported by Huang et al. (2010) were relatively low. Simulated CH_4 emissions for 2002–2003 were much higher than observed. For 2003–2004, CH_4 emission rates were higher for Song et al. (2009) by an approximate magnitude of 2.5 compared to those of Huang et al. (2010). Simulated results were within the range of these two independent studies.

The wetland plant type used in the studies was *Carex lasiocarpa* (Cui, 1997; Wang et al., 2002b; Ding et al., 2004; Hao et al., 2004; Yang et al., 2006). The peak values (growing season) of observed data in a study by Ding et al. (2004) were slightly higher than modelled results for 2001–2002 while the observed data in a study by Hao et al. (2004) were lower than those reported in a study by Ding et al. (2004) as well as this study's simulation for 2002. The model captured the main variations of observations and agreed well with the mean emission of all observations ($R^2 = 0.74$, $D = 0.90$).

For those studies carried out in the Qinghai–Tibet Plateau, modelled peak values were slightly higher than observed data collected from studies with the exception of a 2005 comparison reported in a study by Chen et al. (2008). It was observed that CH_4 emission rates reported by Chen et al. (2008) for 2005 were much higher than their reported 2006 emission rates and also higher than emission rates observed by Wang et al. (2002a) and Ding et al. (2004), even though site locations were situated very close to each other (Fig. 4c, d). By comparing all the observations conducted at Qinghai–Tibet Plateau with the model simulations, the model presented relatively low agreement index ($D = 0.76$) due to the mismatch of peak values.

Data on four natural American wetland sites located in the temperate region were collected. Observational data of Sallie's fen was obtained from the National Center for Ecological Analysis and Synthesis (NCEAS) data repository (Zhuang and Crill, 2008). The remaining observed data were obtained from corresponding citations (Fig. 4e–i) (Burke Jr. et al., 1988; Harriss et al., 1988; Bartlett et al., 1989; Dise, 1993; Shannon and White, 1994; Clement et al., 1995; Wickland et al., 2001). Although the model overestimated or underestimated emission rates for some peak values, Fig. 4e–i show that general seasonal patterns of CH_4 emissions simulated by the model were consistent with observations.

For the site located in north central Minnesota, the mean emission rate was calculated based on observations carried out under different vegetation conditions from a study by Dise (1993). Simulated CH_4 emissions were slightly lower than the observed emissions for winter (Fig. 4e) while modelled results agreed better for static chamber measurement than for eddy correlation measurement (Fig. 4f). The model reached an overall agreement index of 0.91 by combining chamber and eddy correlation data.

For the site located in Michigan, observed CH_4 emissions collected from three individual flux chambers distributed approximately 10 m apart in a study by Shannon and White (1994) were compared to simulated CH_4 emissions on a daily scale for the period 1991–1993 (Fig. 4g). Although the model failed to capture the 1991 summer emission pulse, it performed well for both 1992 and 1993 (Fig. 4g) and showed a good overall agreement index of 0.9.

For the site in a study reported by Wickland et al. (2001), the model again failed to capture peak emissions during the growing season, but it simulated quite well in the remaining

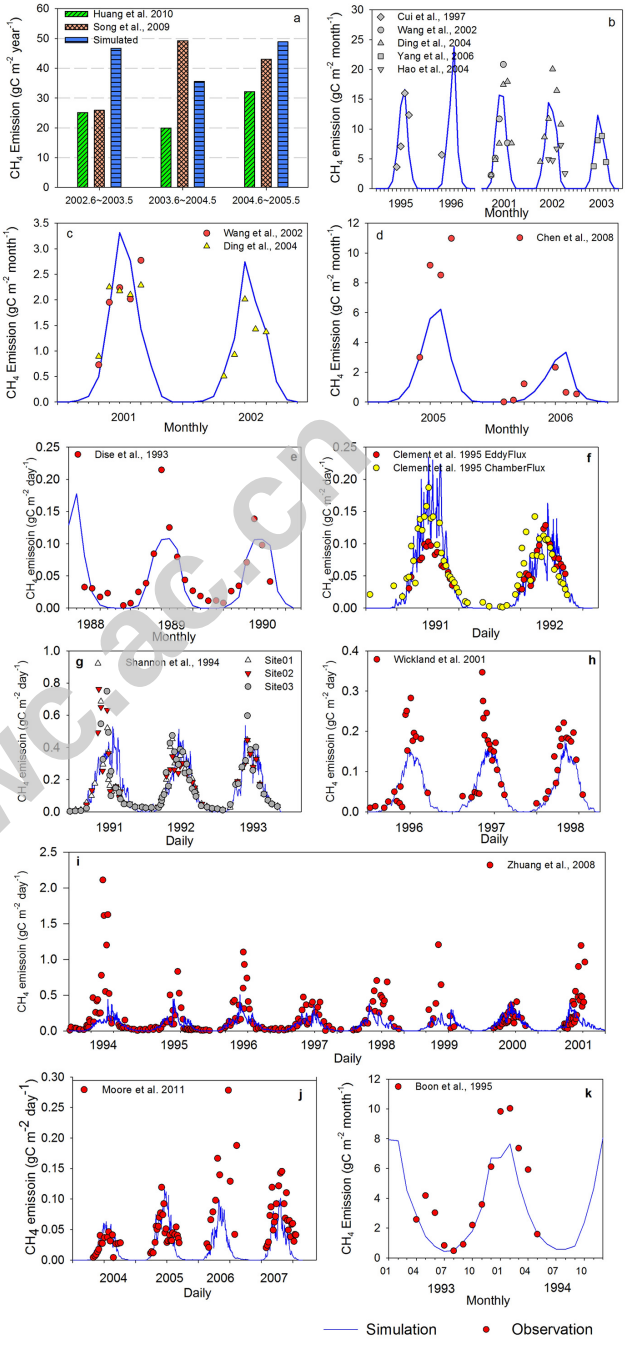

Figure 4. Comparison of modelled and observed CH_4 emissions for the sites located in the temperate region.

seasons (Fig. 4h). Based on the monthly mean emission rates, simulated results agreed well with observations ($R^2 = 0.88$, $D = 0.90$).

For the Sallie's fen site (Zhuang and Crill, 2008), simulated seasonal and annual variation agreed well with an 8-year uninterrupted observation (Fig. 4i). However, it is difficult for the model to capture several peak values during the growing season at this site, especially in 1994 (Fig. 4i), which accounts for the relatively low level of the evaluation index ($R^2 = 0.28$, $D = 0.50$).

In comparison with results reported by Moore et al. (2011), the model underestimated CH_4 emissions from 2006 to 2007, especially in 2006 (note: three observed value points that were much greater than 0.3 gC m^{-2} day^{-1} in 2006 are not shown on the graph), but it agreed well with observations from 2004 and 2005 (Fig. 4j). Overall, in the comparison, the index of agreement is low ($D = 0.42$) because the model did not capture the largest and smallest observations.

Additionally, a set of observed CH_4 emission data related to freshwater wetlands in southeastern Australia was collected from a study by Boon (1995) where field work was carried out over a 14-month period in 1993 and 1994. Seasonal and annual variation patterns for model simulations and observations stood in good agreement with each other (RMSE = 0.05, $R^2 = 0.86$, $D = 0.93$) (Fig. 4k).

4.2.3 Tropical region

Studies carried out in the Florida Everglades have no precise geographical point location; instead, regional averaged modelling results around the Everglades National Park were used for comparison (Fig. 5). Variations in observations ranged from 3.0 mgC m^{-2} day^{-1} to 481.5 mgC m^{-2} day^{-1}. However, the highest emission rate (481.5 mgC m^{-2} day^{-1}) was measured in an open-water site while rapid ebullition was observed on all sampling dates (Burke Jr. et al., 1988). This produced extremely high CH_4 flux at this particular site. Emissions ranged from 3.0 mgC m^{-2} day^{-1} to 186.0 mgC m^{-2} day^{-1} if excluding the open-water site. Based on grid statistics, the simulated mean CH_4 emission for this area was approximately 60.0 mgC m^{-2} day^{-1} with a variation of approximately 20.0 mgC m^{-2} day^{-1}. Modelled emission rate ranges were generally consistent with observed data (Fig. 5a).

Since precise information on field site locations was unavailable for the Amazon Basin, a simple comparison of monthly mean CH_4 emissions was made between mean field observations and regional averaged modelled results (Fig. 5b). Modelled monthly CH_4 emission rates were close to flooded forest emissions rates reported by Bartlett et al. (1988, 1990). Melack et al. (2004) reported that total annual CH_4 emissions from the central Amazon Basin had a mean value of 6.8 TgC yr^{-1}, based on remote sensing estimation. Total emissions for the same area where Melack et al. (2004) carried out their study was evaluated by the current study, based on regional simulations. Modelled annual total emissions were 6.32 TgC yr^{-1}, which was close to the value (6.8) reported by Melack et al. (2004).

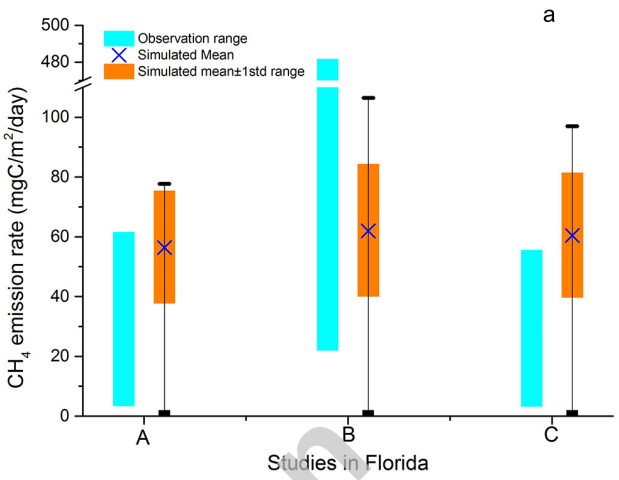

Figure 5a. Comparisons between simulation results of mean (cross symbol) ± 1 SD (orange column) and maximum and minimum (short bar) emission rates and observed emissions range (light blue column) of studies A: Bartlett et al. (1989), B: Burke Jr. et al. (1988), C: Harriss et al. (1988) in Florida everglade.

5 Discussion

Certain assumptions and equations from previous studies and models were adopted by this study in order to construct the CH_4 emission model before being integrated into a DGVM (IBIS) model. Parameters relatively high in model sensitivity were determined through initial sensitivity analysis. Wania et al. (2010) tested seven parameters using more than 2000 different parameter combinations; Riley et al. (2011) tested different parameters for CH_4 production, consumption and transportation processes; Meng et al. (2012) tested eight parameters for sensitivity within certain possible ranges. For this study, only three parameters were selected (r, Q_{10}P, and Q_{10}O) to conduct a series of initial sensitivity analyses. Results show that Q_{10} for CH_4 production had a much higher sensitivity level than Q_{10} for CH_4 oxidation, and the release ratio of CH_4 to CO_2 was highly sensitive to CH_4 emission processes and had direct impacts on CH_4 production. Much stronger temperature dependence during production compared to oxidation was also reported in previous studies (Walter and Heimann, 2000; Walter et al., 2001a; Wania et al., 2010; Riley et al., 2011; Meng et al., 2012), as was the release ratio of CH_4 to CO_2, being the parameter that most influenced CH_4 emissions, with the ratio varying in a large range (Wania et al., 2010; Riley et al., 2011; Spahni et al., 2011; Meng et al., 2012). Therefore, the release ratio of CH_4 to CO_2 and Q_{10} for CH_4 production were selected for

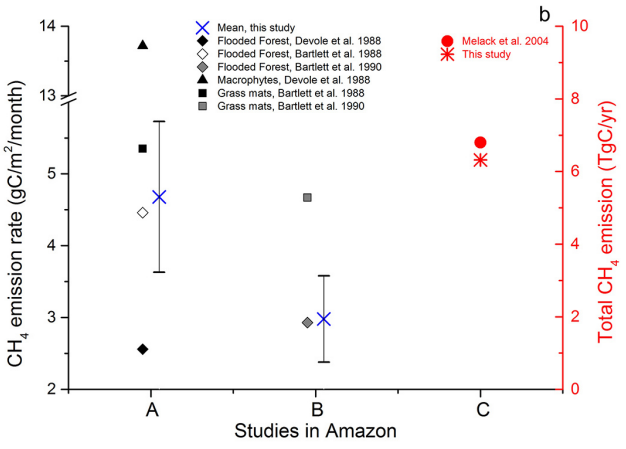

Figure 5b. Comparisons between simulation results of mean (cross symbol) ± 1 SD (short bar) and observations from studies of A: Devol et al. (1988) and Bartlett et al. (1988), and B: Bartlett et al. (1990); C: total annual CH_4 emission comparison between simulation and the study of Melack et al. (2004) in the Amazon.

parameter fitting in order to ascertain the best combination to test model performance and calibrate for individual sites.

Additionally, sensitivity levels indicate that Q_{10}P is much more sensitive in winter than summer for northern middle- to high-latitude regions, while the reverse pattern is observed in tropical regions. Furthermore, Q_{10}P has a higher sensitivity level in boreal and temperate regions than in tropical regions. The gradually increasing parameter Q_{10}P from boreal to temperate to tropical implies that the CH_4 emissions from wetlands are more temperature dependent in high-latitude regions than in the tropical region. Parameter r indicates that the release ratio of CH_4 to CO_2 is higher in the temperate region than the others.

Some simulated results failed to capture peak observed CH_4 emission values during the growing season. The underestimation of CH_4 emission pulse may be partly due to, on the one hand, external environmental triggers and CH_4 contribution from microbial mat systems during summer not being included in the model (Shoemaker and Schrag, 2010; Tian et al., 2010). On the other hand, the ebullition events of short duration, which are often recorded as very high fluxes in the observation, are hard to reproduce (Moore et al., 2011), since some dependent factors (e.g. the density of nucleation site) in CH_4 ebullition process are difficult to simulate (Wania et al., 2010). At the same time, some simulated peak emission values were not seen in the observations. One possible explanation could be the low sampling frequency typical of field work. Although some comparisons were carried out between simulations and observations using the high-frequency eddy covariance technique rather than low-frequency flux chambers, the footprint associated with eddy flux estimation depends on wind properties, boundary layers, surface roughness, etc. (Riley et al., 2011). Nevertheless, the model was able to capture seasonal CH_4 emission variation patterns effectively. For example, a drop in observed emission rates was detected in a study by Rinne et al. (2007) during early July to mid-September. It was suggested that the major reason for this emission drop may be due to the fact that the methanogenic microbe population exceeded growth in available substrates (Rinne et al., 2007). At the same time, the green area of the vascular plants reached its maximum (Rinne et al., 2007), which means that more oxygen can be transported to the tips of the roots of the vascular plants. The subsequently high CH_4 oxidation rate will also contribute to the emission drop. A drop pattern was also found in our simulation during the same period.

Another reason for the differences between simulation and site observations may be attributed to the uncertainties of driving data. For some sites, climate data were obtained from the nearest meteorological station since climate observations in situ were unavailable. The differences of climate condition between modelling sites and meteorological sites could be large due to the effects of topography and geological location. For the model simulations in the tropical region, a global-scale climate data set was used. The climate data set cannot reflect the details of the daily or seasonal variation in temporal and spatial respects for the given large grid. Local climates may differ significantly from grid climates, especially in regions of high relief (Wania et al., 2010). Biases may be subsequently added to simulations of net primary productivity (NPP), heterotrophic respiration, soil water and thermal processes, which are important parameters for CH_4 production. Therefore, it is difficult for the model to capture full emission patterns. The soil property is also difficult to be replicated accurately at site level using a global soil data set, which is also a possible cause for the disagreement between model simulation and observation.

Uncertainties from field observations should also be taken into account in such comparisons. In many studies, for example, observations taken in the first year typically differ from subsequent years. This may be due to the fact that conditions of observational systems are unstable during initial setup. Larger differences are exhibited in the first year between simulations and observations.

It is important to note that two parameter values analysed in this study (r and Q_{10}P) are spatially heterogeneous. For the parameter fitting process, we tried to find the best site-specific parameter combination and to show how well the model can perform at the local site condition. This will continue to be an important issue for model simulation and development at both regional and global scales. Using different parameter sets or an overall uniform parameter set (e.g. average values for all sites) for site-, region- or global-scale simulations should be considered. Collecting more observed CH_4 emissions data sets from different geographic locations and wetland types could produce more reliable parameter sets under different conditions and locations, after which spatial distribution layers for highly sensitive parameters could be

constructed by a specific land surface classification (e.g. wetland types, biome types, etc.), which is something that has not been considered in recent studies (Melton et al., 2013; Wania et al., 2013), but which is important for the evaluation of wetland CH_4 emissions, especially at the regional or global scale. Better parameterization and evaluation of the model can potentially reduce the uncertainties in wetland CH_4 emissions response to projected climate change (Melton et al., 2013).

Further modelling, observational and data collecting works should be carried out to reduce uncertainties and enable more accurate simulations. Firstly, studies have pointed out that CH_4 emissions can be predicted well, but with incorrect contributions of production, oxidation and different transport (Riley et al., 2011; Melton et al., 2013). Further investigation should be conducted to examine methane fluxes from different transport pathways, the proportion of CH_4 production and oxidation, as well as the spatial patterns of these processes across wide geographic locations. Also, support is needed from explicit site observations of CH_4 emission processes, and relative physical and biogeochemical state variables (Melton et al., 2013). Secondly, the site-based simulations indicate that the model struggles to capture the peak emissions that are largely contributed by ebullition process. Though the process is hard to predict, preliminary improvement should be considered in the next stage. For example, a lower threshold could be used in the growing season, thus with higher ebullition (Spahni et al., 2011). Thirdly, in this current study, only one PFT was added for wetlands without considering specific wetland plants type (e.g. graminoids, sedges, sphagnum, moss). The model could be improved by considering the spatial characteristics of wetland vegetation, as well as including different effects of vascular and nonvascular plants on CH_4 emissions processes, especially for the oxidation and plant-mediated transport processes. Fourthly, CH_4 oxidation rate was simulated as a function of CH_4 concentration, soil temperature and soil redox potential in this study. Redox potential was used to represent the condition of soil electron acceptor. Although methane oxidation can happen under anaerobic conditions with available alternative electron acceptors (Zhuang et al., 2004), modelling dynamic changes of oxygen in the profile, including diffusion through soil layers and transport from atmosphere via vascular plants, is essential in the methanotrophic process (Wania et al., 2010). These processes need to be considered explicitly in further model development. Finally, more data from literature reviews or field measurements are needed to conduct the parameterization of the water table module and test model simulation performance, because the water table is an important factor controlling CH_4 production, consumption and transportation processes.

6 Summary and conclusions

This study has introduced the successful integration of a CH_4 biogeochemistry module incorporating CH_4 production, oxidation and transportation processes into an existing DGVM (IBIS). Factors controlling CH_4 emission processes, such as soil temperature, redox potential and pH, were specified into the model. A water table module was also integrated into DGVM to improve hydrological processes for wetland simulation. Sensitivity analysis indicates that the release ratio of CH_4 to CO_2 and Q_{10} for CH_4 production are two major controlling factors in CH_4 emission modelling. These two parameters were subsequently calibrated to data obtained from 19 sites collected from approximately 35 studies across different wetlands globally, which is a more extensive sampling than previous models have encompassed. Having a heterogeneous spatial distribution, r ranged from 0.1 to 0.7 with a mean value of 0.23, and the Q_{10} for CH_4 production ranged from 1.6 to 4.5 with a mean value of 2.48. We found that the TRIPLEX-GHG was able to capture patterns in temporal variation of CH_4 emission, but was unable to simulate daily details or the emission pulse. Results suggest that the TRIPLEX-GHG model can be applied to different wetlands under varying conditions. It should contribute to the scientific modelling community by accounting for GHG exchange and the budgeting of terrestrial ecosystems, especially the CH_4 budget at both regional and global scales.

Acknowledgements. This study was funded by the National Basic Research Programme of China (2013CB956602), the National Natural Science Foundation of China (41201079), the Programme of NCET, the Start-up Funds (Z111021203) and Basic Research Funds (Z109021204) of Northwest A&F University, the Specialized Research Fund for the Doctoral Programme of Higher Education of China (20120204120007), and the Natural Sciences and Engineering Research Council of Canada Discovery Grant. The authors would like to thank three anonymous reviewers for their valuable comments and constructive suggestions which greatly improved the paper.

Edited by: A. Stenke

References

Arneth, A., Sitch, S., Bondeau, A., Butterbach-Bahl, K., Foster, P., Gedney, N., de Noblet-Ducoudré, N., Prentice, I. C., Sanderson, M., Thonicke, K., Wania, R., and Zaehle, S.: From biota to chemistry and climate: towards a comprehensive description of trace gas exchange between the biosphere and atmosphere, Biogeosciences, 7, 121–149, doi:10.5194/bg-7-121-2010, 2010.

Bartlett, D. S., Bartlett, K. B., Hartman, J. M., Harriss, R. C., Sebacher, D. I., Pelletier-Travis, R., Dow, D. D., and Brannon, D. P.: Methane emissions from the Florida Everglades: Patterns of variability in a regional wetland ecosystem, Global Biogeochem. Cy., 3, 363–374, doi:10.1029/GB003i004p00363, 1989.

Bartlett, K. B., Crill, P. M., Sebacher, D. I., Harriss, R. C., Wilson, J. O., and Melack, J. M.: Methane Flux From the Central Amazonian Floodplain, J. Geophys. Res., 93, 1571–1582, doi:10.1029/JD093iD02p01571, 1988.

Bartlett, K. B., Crill, P. M., Bonassi, J. A., Richey, J. E., and Harriss, R. C.: Methane flux from the Amazon River floodplain: emissions during rising water, J. Geophys. Res., 95, 16773–16788, 1990.

Batjes, N. H.: ISRIC-WISE derived soil properties on a 5 by 5 arcminutes global grid, Report 2006/02, available at: http://www.isric.org (last access: 9 May 2014), ISRIC-World Soil Information, Wageningen (with data set), 2006.

Boon, P. I.: Methanogenesis in the sediments of an Australian freshwater wetland: Comparison with aerobic decay, and factors controlling methanogenesis, Fems Microbiol. Ecol., 18, 175–190, doi:10.1016/0168-6496(95)00053-5, 1995.

Burke Jr., R. A., Barber, T. R., and Sackett, W. M.: Methane flux and stable hydrogen and carbon isotope composition of sedimentary methane from the Florida Everglades, Global Biogeochem. Cy., 2, 329–340, doi:10.1029/GB002i004p00329, 1988.

Cao, M., Dent, J. B., and Heal, O. W.: Modeling methane emissions from rice paddies, Global Biogeochem. Cy., 9, 183–195, doi:10.1029/94gb03231, 1995.

Cao, M., Marshall, S., and Gregson, K.: Global carbon exchange and methane emissions from natural wetlands: Application of a process-based model, J. Geophys. Res.-Atmos., 101, 14399–14414, 1996.

Chen, H., Yao, S., Wu, N., Wang, Y., Luo, P., Tian, J., Gao, Y., and Sun, G.: Determinants influencing seasonal variations of methane emissions from alpine wetlands in Zoige Plateau and their implications, J. Geophys. Res., 113, D12303, doi:10.1029/2006jd008072, 2008.

Chen, H., Zhu, Q., Peng, C., Wu, N., Wang, Y., Fang, X., Jiang, H., Xiang, W., Chang, J., Deng, X., and Yu, G.: Methane emissions from rice paddies natural wetlands, and lakes in China: synthesis and new estimate, Glob. Change Biol., 19, 19–32, doi:10.1111/gcb.12034, 2013.

Chen, Y. H. and Prinn, R. G.: Atmospheric modeling of high- and low-frequency methane observations: Importance of interannually varying transport, J. Geophys. Res.-Atmos., 110, D10303, doi:10.1029/2004jd005542, 2005.

Ciais, P., Sabine, C., Bala, G., Bopp, L., Brovkin, V., Canadell, J., Chhabra, A., DeFries, R., Galloway, J., Heimann, M., Jones, C., Quéré, C. L., Myneni, R. B., Piao, S., and Thornton, P.: Carbon and Other Biogeochemical Cycles, Cambridge University Press, Cambridge, United Kingdom and New York, NY, USA, 465–570, 2013.

Clement, R. J., Verma, S. B., and Verry, E. S.: Relating Chamber Measurements to Eddy-Correlation Measurements of Methane Flux, J. Geophys. Res.-Atmos., 100, 21047–21056, 1995.

Cramer, W., Bondeau, A., Woodward, F. I., Prentice, I. C., Betts, R. A., Brovkin, V., Cox, P. M., Fisher, V., Foley, J. A., Friend, A. D., Kucharik, C., Lomas, M. R., Ramankutty, N., Sitch, S., Smith, B., White, A., and Young-Molling, C.: Global response of terrestrial ecosystem structure and function to CO_2 and climate change: results from six dynamic global vegetation models, Glob. Change. Biol., 7, 357–373, 2001.

Cui, B.: Estimation of CH_4 emission from Sanjiang plain, scientia Geographica Sinica, 17, 93–95, 1997 (in Chinese with English abstract).

Devol, A. H., Richey, J. E., Clark, W. A., King, S. L., and Martinelli, L. A.: Methane emissions to the troposphere from the Amazon floodplain, J. Geophys. Res., 93, 1583–1592, 1988.

Ding, W., Cai, Z., and Wang, D.: Preliminary budget of methane emissions from natural wetlands in China, Atmos. Environ., 38, 751–759, doi:10.1016/j.atmosenv.2003.10.016, 2004.

Dise, N. B.: Winter Fluxes of Methane from Minnesota Peatlands, Biogeochemistry, 17, 71–83, 1992.

Dise, N. B.: Methane Emission from Minnesota Peatlands – Spatial and Seasonal Variability, Global Biogeochem. Cy., 7, 123–142, 1993.

Dunfield, P., Knowles, R., Dumont, R., and Moore, T. R.: Methane production and consumption in temperate and subarctic peat soils: Response to temperature and pH, Soil Biol. Biochem., 25, 321–326, 1993.

Enting, I., Heimann, M., and Wigley, T.: Future emissions and concentrations of carbon dioxide: Key ocean/atmosphere/land analyses, CSIRO Division of Atmospheric Research Technical Paper No. 31, CSIRO, Australia, 1994.

EPA: Methane-and-Nitrous-Oxide-Emissions-From-Natural-Sources, Washington, DC 20460, 2010.

Fiedler, S. and Sommer, M.: Methane emissions, groundwater levels and redox potentials of common wetland soils in a temperate-humid climate, Global Biogeochem. Cy., 14, 1081–1093, doi:10.1029/1999gb001255, 2000.

Foley, J. A., Colin, P. I., Ramankutty, N., Levis, S., Pollard, D., Sitch, S., and Haxeltine, A.: An integrated biosphere model of land surface processes, terrestrial carbon balance, and vegetation dynamics, Global Biogeochem. Cy., 10, 603–628, 1996.

Frolking, S. and Crill, P.: Climate Controls on Temporal Variability of Methane Flux from a Poor Fen in Southeastern New-Hampshire – Measurement and Modeling, Global Biogeochem. Cy., 8, 385–397, doi:10.1029/94gb01839, 1994.

Gedney, N., Cox, P. M., and Huntingford, C.: Climate feedback from wetland methane emissions, Geophys. Res. Lett., 31, L20503, doi:10.1029/2004gl020919, 2004.

Granberg, G., Grip, H., Ottosson Löfvenius, M., Sundh, I., Svensson, B. H., and Nilsson, M.: A simple model for simulation of water content, soil frost, and soil temperatures in boreal mixed mires, Water. Resour. Res., 35, 3771–3782, doi:10.1029/1999wr900216, 1999.

Granberg, G., Ottosson-Lofvenius, M., Grip, H., Sundh, I., and Nilsson, M.: Effect of climatic variability from 1980 to 1997 on simulated methane emission from a boreal mixed mire in northern Sweden, Global Biogeochem. Cy., 15, 977–991, 2001.

Hao, Q., Wang, Y., Song, C., Liu, G., Wang, Y., and Wang, M.: Study of CH_4 Emission From Wetlands in Sanjiang Plain, J. Soil Water Conserv., 18, 194–199, 2004 (in Chinese with English abstract).

Harriss, R. C., Sebacher, D. I., Bartlett, K. B., Bartlett, D. S., and Crill, P. M.: Sources of atmospheric methane in the south Florida environment, Global Biogeochem. Cy., 2, 231–243, doi:10.1029/GB002i003p00231, 1988.

Hartmann, D. L., Tank, A. M. G. K., Rusticucci, M., Alexander, L. V., Brönnimann, S., Charabi, Y., Dentener, F. J., Dlugokencky, E. J., Easterling, D. R., Kaplan, A., Soden, B. J., Thorne, P. W.,

Wild, M., and Zhai, P. M.: Observations: Atmosphere and Surface, Cambridge University Press, Cambridge, United Kingdom and New York, NY, USA, 165–179, 2013.

Huang, Y., Sun, W. J., Zhang, W., Yu, Y. Q., Su, Y. H., and Song, C. C.: Marshland conversion to cropland in northeast China from 1950 to 2000 reduced the greenhouse effect, Glob. Change Biol., 16, 680–695, doi:10.1111/j.1365-2486.2009.01976.x, 2010.

Ito, A. and Inatomi, M.: Use of a process-based model for assessing the methane budgets of global terrestrial ecosystems and evaluation of uncertainty, Biogeosciences, 9, 759–773, doi:10.5194/bg-9-759-2012, 2012.

Jackowicz-Korczyński, M., Christensen, T. R., Bäckstrand, K., Crill, P., Friborg, T., Mastepanov, M., and Ström, L.: Annual cycle of methane emission from a subarctic peatland, J. Geophys. Res., 115, G02009, doi:10.1029/2008jg000913, 2010.

Keeling, C. D., Piper, S. C., Bacastow, R. B., Wahlen, M., Whorf, T. P., Heimann, M., and Meijer, H. A.: Atmospheric CO_2 and $^{13}CO_2$ exchange with the terrestrial biosphere and oceans from 1978 to 2000: observations and carbon cycle implications, in: A History of Atmospheric CO_2 and its effects on Plants Animals and Ecosystems, edited by: Ehleringer, J. R., Cerling, T. E., and Dearing, M. D., Springer Verlag, New York, 83–113, 2005.

Kirschke, S., Bousquet, P., Ciais, P., Saunois, M., Canadell, J. G., Dlugokencky, E. J., Bergamaschi, P., Bergmann, D., Blake, D. R., Bruhwiler, L., Cameron-Smith, P., Castaldi, S., Chevallier, F., Feng, L., Fraser, A., Heimann, M., Hodson, E. L., Houweling, S., Josse, B., Fraser, P. J., Krummel, P. B., Lamarque, J.-F., Langenfelds, R. L., Le Quere, C., Naik, V., O'Doherty, S., Palmer, P. I., Pison, I., Plummer, D., Poulter, B., Prinn, R. G., Rigby, M., Ringeval, B., Santini, M., Schmidt, M., Shindell, D. T., Simpson, I. J., Spahni, R., Steele, L. P., Strode, S. A., Sudo, K., Szopa, S., van der Werf, G. R., Voulgarakis, A., van Weele, M., Weiss, R. F., Williams, J. E., and Zeng, G.: Three decades of global methane sources and sinks, Nat. Geosci., 6, 813–823, doi:10.1038/ngeo1955, 2013.

Kucharik, C. J., Foley, J. A., Delire, C., Fisher, V. A., Coe, M. T., lenters, J. D., Young-Molling, C., and Ramankutty, N.: Testing the performance of a Dynamic Global Ecosystem Model: Water balance, carbon balance, and vegetation structure, Global Biogeochem. Cy., 14, 795–825, 2000.

Kucharik, C. J., Barford, C. C., El Maayar, M., Wofsy, S. C., Monson, R. K., and Baldocchi, D. D.: A multiyear evaluation of a Dynamic Global Vegetation Model at three AmeriFlux forest sites: Vegetation structure, phenology, soil temperature, and CO_2 and H_2O vapor exchange, Ecol. Model., 196, 1–31, doi:10.1016/j.ecolmodel.2005.11.031, 2006.

Lenhart, T., Eckhardt, K., Fohrer, N., and Frede, H.-G.: Comparison of two different approaches of sensitivity analysis, Phys. Chem. Earth, 27, 645–654, 2002.

Li, C. S.: Modeling Trace Gas Emissions from Agricultural Ecosystems, Nutr. Cycl. Agroecosys., 58, 259–276, doi:10.1023/a:1009859006242, 2000.

Liu, J., Price, D., and Chen, J.: Nitrogen controls on ecosystem carbon sequestration: a model implementation and application to Saskatchewan, Canada, Ecol. Model., 186, 178–195, doi:10.1016/j.ecolmodel.2005.01.036, 2005.

Ma, K., You, L., Liu, J., and Zhang, M.: A Hybrid Wetland Map for China: A Synergistic Approach Using Census and Spatially Explicit Datasets, Plos One, 7, e47814, doi:10.1371/journal.pone.0047814, 2012.

Melack, J. M., Hess, L. L., Gastil, M., Forsberg, B. R., Hamilton, S. K., Lima, I. B. T., and Novo, E. M. L. M.: Regionalization of methane emissions in the Amazon Basin with microwave remote sensing, Glob. Change. Biol., 10, 530–544, doi:10.1111/j.1365-2486.2004.00763.x, 2004.

Melloh, R. A. and Crill, P. M.: Winter methane dynamics in a temperate peatland, Global Biogeochem. Cy., 10, 247–254, 1996.

Melton, J. R., Wania, R., Hodson, E. L., Poulter, B., Ringeval, B., Spahni, R., Bohn, T., Avis, C. A., Beerling, D. J., Chen, G., Eliseev, A. V., Denisov, S. N., Hopcroft, P. O., Lettenmaier, D. P., Riley, W. J., Singarayer, J. S., Subin, Z. M., Tian, H., Zürcher, S., Brovkin, V., van Bodegom, P. M., Kleinen, T., Yu, Z. C., and Kaplan, J. O.: Present state of global wetland extent and wetland methane modelling: conclusions from a model intercomparison project (WETCHIMP), Biogeosciences, 10, 753–788, doi:10.5194/bg-10-753-2013, 2013.

Meng, L., Hess, P. G. M., Mahowald, N. M., Yavitt, J. B., Riley, W. J., Subin, Z. M., Lawrence, D. M., Swenson, S. C., Jauhiainen, J., and Fuka, D. R.: Sensitivity of wetland methane emissions to model assumptions: application and model testing against site observations, Biogeosciences, 9, 2793–2819, doi:10.5194/bg-9-2793-2012, 2012.

Moore, T. R. and Knowles, R.: Methane Emissions from Fen, Bog and Swamp Peatlands in Quebec, Biogeochemistry, 11, 45–61, 1990.

Moore, T. R., De Young, A., Bubier, J. L., Humphreys, E. R., Lafleur, P. M., and Roulet, N. T.: A Multi-Year Record of Methane Flux at the Mer Bleue Bog, Southern Canada, Ecosystems, 14, 646–657, doi:10.1007/s10021-011-9435-9, 2011.

Myhre, G., Shindell, D., Bréon, F.-M., Collins, W., Fuglestvedt, J., Huang, J., Koch, D., J.-F. Lamarque, D., Lee, B. M., Nakajima, T., Robock, A., Stephens, G., Takemura, T., and Zhang, H.: Anthropogenic and Natural Radiative Forcing, Cambridge University Press, Cambridge, United Kingdom and New York, NY, USA, 731–738, 2013.

Nisbet, E. G., Dlugokencky, E. J., and Bousquet, P.: Methane on the rise – again, Science, 343, 493–495, doi:10.1126/science.1247828, 2014.

Ojima, D. S., Holland, E. A., Melillo, J. M., Mosier, A. R., and Robertson, G. P.: TRAGNET Workshop Report: Building a U.S. Trace Gas Network, Pingree Park, Colorado, USA, 1992.

Panikov, N. S. and Dedysh, S. N.: Cold season CH_4 and CO_2 emission from boreal peat bogs (West Siberia): Winter fluxes and thaw activation dynamics, Global Biogeochem. Cy., 14, 1071–1080, 2000.

Pelletier, L., Moore, T. R., Roulet, N. T., Garneau, M., and Beaulieu-Audy, V.: Methane fluxes from three peatlands in the La Grande Riviere watershed, James Bay lowland, Canada, J. Geophys. Res.-Biogeo., 112, G01018, doi:10.1029/2006jg000216, 2007.

Peng, C., Liu, J., Dang, Q., Apps, M. J., and Jiang, H.: TRIPLEX: A generic hybrid model for predicting forest growth and carbon and nitrogen dynamics, Ecol. Model., 153, 109–130, doi:10.1016/s0304-3800(01)00505-1, 2002.

Peng, C. H., Liu, J. X., Zhu, Q. A., and Chen, H.: Framework for Integrating greenhouse gas emission processes into a dynamic

global vegetation model: TRIPLEX-GHG model development and testing, North America Carbon Program, New Mexico, 2013.

Petrescu, A. M. R., van Beek, L. P. H., van Huissteden, J., Prigent, C., Sachs, T., Corradi, C. A. R., Parmentier, F. J. W., and Dolman, A. J.: Modeling regional to global CH_4 emissions of boreal and arctic wetlands, Global Biogeochem. Cy., 24, GB4009, doi:10.1029/2009gb003610, 2010.

Prentice, I. C., Webb, R. S., Ter-Mikhaelian, M. T., Solomon, A. M., Smith, T. M., Pitovranov, S. E., Nikolov, N. T., Minin, A. A., Leemans, R., Lavorel, S., Korzukhin, M. D., Hrabovszky, J. P., Helmisaari, H. O., Harrison, S. P., Emanuel, W. R., and Bonan, G. B.: Developing a global vegetation dynamics model : results of an IIASA summer workshop, Laxenburg, Austria, 52 pp., 1989.

Riley, W. J., Subin, Z. M., Lawrence, D. M., Swenson, S. C., Torn, M. S., Meng, L., Mahowald, N. M., and Hess, P.: Barriers to predicting changes in global terrestrial methane fluxes: analyses using CLM4Me, a methane biogeochemistry model integrated in CESM, Biogeosciences, 8, 1925–1953, doi:10.5194/bg-8-1925-2011, 2011.

Rinne, J., Riutta, T., Pihlatie, M., Aurela, M., Haapanala, S., Tuovinen, J. P., Tuittila, E. S., and Vesala, T.: Annual cycle of methane emission from a boreal fen measured by the eddy covariance technique, Tellus B, 59, 449–457, doi:10.1111/j.1600-0889.2007.00261.x, 2007.

Saarnio, S., Alm, J., Silvola, J., Lohila, A., Nykänen, H., and Martikainen, P. J.: Seasonal variation in CH_4 emissions and production and oxidation potentials at microsites on an oligotrophic pine fen, Oecologia, 110, 414–422, doi:10.1007/s004420050176, 1997.

Sass, R. L., Fisher, F. M., Harcombe, P. A., and Turner, F. T.: Methane production and emission in a Texas rice field, Global Biogeochem. Cy., 4, 47–68, doi:10.1029/GB004i001p00047, 1990.

Segers, R.: Methane Production and Methane Consumption: A Review of Processes Underlying Wetland Methane Fluxes, Biogeochemistry, 41, 23–51, 1998.

Sellers, P. J., Hall, F. G., Kelly, R. D., Black, A., Baldocchi, D., Berry, J., Ryan, M., Ranson, K. J., Crill, P. M., Lettenmaier, D. P., Margolis, H., Cihlar, J., Newcomer, J., Fitzjarrald, D., Jarvis, P. G., Gower, S. T., Halliwell, D., Williams, D., Goodison, B., Wickland, D. E., and Guertin, F. E.: BOREAS in 1997: Experiment overview, scientific results, and future directions, J. Geophys. Res.-Atmos., 102, 28731–28769, 1997.

Shannon, R. D. and White, J. R.: A Three-Year Study of Controls on Methane Emissions from Two Michigan Peatlands, Biogeochemistry, 27, 35–60, 1994.

Shannon, R. D., White, J. R., Lawson, J. E., and Gilmour, B. S.: Methane efflux from emergent vegetation in peatlands, J. Ecol., 84, 239–246, 1996.

Shindell, D. T., Walter, B. P., and Faluvegi, G.: Impacts of climate change on methane emissions from wetlands, Geophys. Res. Lett., 31, L21202, doi:10.1029/2004gl021009, 2004.

Shoemaker, J. K. and Schrag, D. P.: Subsurface characterization of methane production and oxidation from a New Hampshire wetland, Geobiology, 8, 234–243, doi:10.1111/j.1472-4669.2010.00239.x, 2010.

Song, C., Xu, X., Tian, H., and Wang, Y.: Ecosystem-atmosphere exchange of CH_4 and N_2O and ecosystem respiration in wetlands in the Sanjiang Plain, Northeastern China, Glob. Change Biol., 15, 692–705, doi:10.1111/j.1365-2486.2008.01821.x, 2009.

Spahni, R., Wania, R., Neef, L., van Weele, M., Pison, I., Bousquet, P., Frankenberg, C., Foster, P. N., Joos, F., Prentice, I. C., and van Velthoven, P.: Constraining global methane emissions and uptake by ecosystems, Biogeosciences, 8, 1643–1665, doi:10.5194/bg-8-1643-2011, 2011.

Stocker, B. D., Roth, R., Joos, F., Spahni, R., Steinacher, M., Zaehle, S., Bouwman, L., Xu, R., and Prentice, I. C.: Multiple greenhouse-gas feedbacks from the land biosphere under future climate change scenarios, Nature Climate Change, 3, 666–672, doi:10.1038/nclimate1864, 2013.

Strom, L., Mastepanov, M., and Christensen, T. R.: Species-specific effects of vascular plants on carbon turnover and methane emissions from wetlands, Biogeochemistry, 75, 65–82, 2005.

Svensson, B. H., Christensen, T. R., Johansson, E., and Oquist, M.: Interdecadal changes in CO_2 and CH_4 fluxes of a subarctic mire: Stordalen revisited after 20 years, Oikos, 85, 22–30, 1999.

Tian, H., Xu, X., Liu, M., Ren, W., Zhang, C., Chen, G., and Lu, C.: Spatial and temporal patterns of CH_4 and N_2O fluxes in terrestrial ecosystems of North America during 1979–2008: application of a global biogeochemistry model, Biogeosciences, 7, 2673–2694, doi:10.5194/bg-7-2673-2010, 2010.

Valentine, D. W., Holland, E. A., and Schinel, D. S.: Ecosystem and physical controls over methane production in northern wetlands, J. Geophys. Res., 99, 1563–1571, 1994.

van Huissteden, J., van den Bos, R., and Alvarez, I. M.: Modelling the effect of water-table management on CO_2 and CH_4 fluxes from peat soils, Netherlands Journal of Geosciences, 85, 3–18, 2006.

Walter, B. P. and Heimann, M.: A process-based, climate-sensitive model to derive methane emissions from natural wetlands: Application to five wetland sites, sensitivity to model parameters, and climate, Global Biogeochem. Cy., 14, 745–765, doi:10.1029/1999gb001204, 2000.

Walter, B. P., Heimann, M., and Matthews, E.: Modeling modern methane emissions from natural wetlands 2. Interannual variations 1982–1993, J. Geophys. Res., 106, 34207–34219, doi:10.1029/2001jd900164, 2001a.

Walter, B. P., Heimann, M., and Matthews, E.: Modeling modern methane emissions from natural wetlands 1. Model description and results, J. Geophys. Res., 106, 34189–34206, doi:10.1029/2001jd900165, 2001b.

Wang, D., Lu, X., Ding, W., Cai, Z., Gao, J., and Yang, F.: Methane emission from marshes in Zoige Plateau, Adv. Earth Sci., 17, 877–880, 2002a.

Wang, D., Lu, X., Ding, W., Cai, Z., and Wang, Y.: Comparison of Methane Emission from Marsh and Paddy Field in Sanjiang Plain, Scientia Geographica Sinica, 22, 500–503, 2002b (in Chinese with English abstract).

Wang, Y. P., Law, R. M., and Pak, B.: A global model of carbon, nitrogen and phosphorus cycles for the terrestrial biosphere, Biogeosciences, 7, 2261–2282, doi:10.5194/bg-7-2261-2010, 2010.

Wang, Z. P., Delaune, R. D., Masscheleyn, P. H., and Patrick, W. H.: Soil Redox and Ph Effects on Methane Production in a Flooded Rice Soil, Soil Sci. Soc. Am. J., 57, 382–385, 1993.

Wania, R., Ross, I., and Prentice, I. C.: Integrating peatlands and permafrost into a dynamic global vegetation model: 2. Evaluation and sensitivity of vegetation and car-

bon cycle processes, Global. Biogeochem. Cy., 23, GB3015, doi:10.1029/2008gb003413, 2009a.

Wania, R., Ross, I., and Prentice, I. C.: Integrating peatlands and permafrost into a dynamic global vegetation model: 1. Evaluation and sensitivity of physical land surface processes, Global. Biogeochem. Cy., 23, GB3014, doi:10.1029/2008gb003412, 2009b.

Wania, R., Ross, I., and Prentice, I. C.: Implementation and evaluation of a new methane model within a dynamic global vegetation model: LPJ-WHyMe v1.3.1, Geosci. Model Dev., 3, 565–584, doi:10.5194/gmd-3-565-2010, 2010.

Wania, R., Melton, J. R., Hodson, E. L., Poulter, B., Ringeval, B., Spahni, R., Bohn, T., Avis, C. A., Chen, G., Eliseev, A. V., Hopcroft, P. O., Riley, W. J., Subin, Z. M., Tian, H., van Bodegom, P. M., Kleinen, T., Yu, Z. C., Singarayer, J. S., Zürcher, S., Lettenmaier, D. P., Beerling, D. J., Denisov, S. N., Prigent, C., Papa, F., and Kaplan, J. O.: Present state of global wetland extent and wetland methane modelling: methodology of a model inter-comparison project (WETCHIMP), Geosci. Model Dev., 6, 617–641, doi:10.5194/gmd-6-617-2013, 2013.

Weiss, R., Shurpali, N. J., Sallantaus, T., Laiho, R., Laine, J., and Alm, J.: Simulation of water table level and peat temperatures in boreal peatlands, Ecol. Model., 192, 441–456, doi:10.1016/j.ecolmodel.2005.07.016, 2006.

Westermann, P.: Temperature regulation of methanogenesis in wetlands, Chemosphere, 26, 321–328, 1993.

Whalen, S. C. and Reeburgh, W. S.: Interannual variations in tundra methane emission: A 4-year time series at fixed sites, Global Biogeochem. Cy., 6, 139–159, doi:10.1029/92gb00430, 1992.

Whiting, G. J. and Chanton, J. P.: Primary Production Control of Methane Emission from Wetlands, Nature, 364, 794–795, 1993.

Wickland, K. P., Striegl, R. G., Mast, M. A., and Clow, D. W.: Interannual variation of soil respiration in two New England forests, Global Biogeochem Cy., 15, 321–335, doi:10.1029/2000gb001325, 2001.

Willmott, C. J.: On the Validation of Models, Phys. Geogr., 2, 184–194, 1981.

Yang, J., Liu, J., Wang, J., Yu, J., Sun, Z., and Li, X.: Emissions of CH_4 and N_2O from a wetland in the Sanjiang plain, J. Plant Ecol., 30, 432–440, 2006 (in Chinese with English abstract).

Zhang, Y., Li, C. S., Trettin, C. C., Li, H., and Sun, G.: An integrated model of soil, hydrology, and vegetation for carbon dynamics in wetland ecosystems, Global Biogeochem. Cy., 16, 1061, doi:10.1029/2001gb001838, 2002.

Zhuang, Q. and Crill, P.: NCEAS 10645: Toward an adequate quantification of CH_4 emissions from land ecosystems: Integrating field and in-situ observations, satellite data, and modeling. Sallies Fen NH CH_4 Flux 1994–2001, National Center for Ecological Analysis and Synthesis and Stockholm University, 2008.

Zhuang, Q., Melillo, J. M., Kicklighter, D. W., Prinn, R. G., McGuire, A. D., Steudler, P. A., Felzer, B. S., and Hu, S.: Methane fluxes between terrestrial ecosystems and the atmosphere at northern high latitudes during the past century: A retrospective analysis with a process-based biogeochemistry model, Global Biogeochem. Cy., 18, GB3010, doi:10.1029/2004gb002239, 2004.